Title

Interferon-β induction heterogeneity during KSHV infection is correlated to expression and activation of enhanceosome transcription factors other than IRF3

Running Title

Interferon-β heterogeneity during KSHV infection

Authors

Machika Kaku[a,b] and Marta Maria Gaglia[b, #]

[a]Program in Immunology, Tufts Graduate School of Biomedical Sciences, Boston, MA

[b]Department of Medical Microbiology and Immunology, Institute for Molecular Virology, and Carbone Cancer Center, University of Wisconsin - Madison, WI

ORCIDs: 0000-0002-9921-0678 (M.K.); 0000-0002-1791-0663 (M.M.G.)

[#]Correspondence and reprint requests to Dr. Marta Gaglia, University of Wisconsin-Madison, 1525 Linden Dr, Madison, WI 53706. E-mail address: marta.gaglia@wisc.edu. Phone number: (608)263-5551

Word counts: abstract – 152, importance – 148, text – 6911

Abstract

Strict regulation of type I interferons (IFN) is vital for balancing tissue damage and protection against infections. We previously found that during Kaposi's sarcoma-associated herpesvirus infection, type I IFN induction was limited to a small percentage of infected cells. This heterogeneity was not explained by viral gene expression. Here, we used a fluorescent reporter and fluorescence activated cell sorting to investigate the source of this heterogeneity. Surprisingly, the canonical IFN induction pathway culminating in the activation of the IRF3 transcription factor was similarly activated between cells that made high vs. low/no IFN-β. In contrast, the activation or expression of the two other IFN transcription factors, NF-κB and AP-1, correlated with IFN-β induction. Our results suggest that during viral infection, activation of IRF3 does not automatically result in IFN responses at the level of individual cells, but that other factors, such as NF-κB and AP-1, are limiting for type I IFN induction.

35 **Importance**

36 The ability of mammalian cells to react to viral infections is a crucial step in the
37 induction of immune responses. The first course of action for the cell is to express and
38 release type I interferons like interferon-β (IFN-β), secreted molecules that warn
39 surrounding cells. Single-cell level examination of gene expression has revealed that
40 surprisingly, during many viral infections, only a small fraction of infected cells makes
41 IFN-β. This is likely a mechanism to prevent immune system overreactions. However, it
42 remains unclear why only some cells respond. Here, we find that during infection with
43 Kaposi's sarcoma-associated herpesvirus, an oncogenic virus that affects
44 immunocompromised individuals, the transcription factors AP-1 and NF-κB, rather than
45 the more commonly studied IRF3, may decide which cells go on to make IFN-β. Our
46 findings contribute to a better understanding of complex gene regulation and shed light
47 on a process that fights an oncogenic virus.

48 **Introduction**

49 Type I and III interferons (IFNs) such as interferon-β (IFN-β) and interferon-λs
50 (IFN-λ) are potent cytokines that defend mammals against viral infections. As a key
51 component of innate immunity, they are induced in response to pathogen-associated
52 molecular patterns (PAMPs), such as nucleic acids with unfamiliar characteristics, or
53 damage-associated molecular patterns (DAMPs) due to infection-induced stress.
54 PAMPs and DAMPs are sensed by pattern recognition receptors (PRRs), leading to IFN
55 induction. Type I and III IFNs then orchestrate antiviral defense by signaling through the
56 IFNAR1/2 and IFNLR1/IL10Rβ receptor complexes, respectively, and induce hundreds
57 of interferon stimulated genes (ISGs) (1). ISGs encode proteins that alter cell physiology
58 to antagonize viral replication (2). Despite this crucial antiviral role, IFNs are well known
59 to be a double-edged sword because of their powerful effects on cell and tissue
60 physiology. While insufficient IFN-related inflammation leaves the host susceptible to
61 infections, excessive IFN-related inflammation causes tissue damage and contributes to
62 autoimmune disease development (3-5). Therefore, IFN-β and other type I and III IFNs
63 are carefully regulated, and multiple host regulatory mechanisms have evolved to
64 ensure their expression only under appropriate conditions.

65 An emerging dimension of IFN regulation is transcriptional heterogeneity at the
66 single cell level. This aspect of interferon regulation has become clear from the growing
67 number of single cell RNA sequencing (scRNA-seq) analyses of infected cells. We and
68 others have found only a small percentage (<10%) of virus-infected cells produce IFN-β
69 or IFN-λ (6-18). This has been reported in infections with the RNA viruses Influenza A
70 Virus (7, 10, 11, 14-17), Newcastle Disease Virus (18, 19), West Nile Virus (13), and

71 SARS-CoV-2 (9), as well as the DNA viruses Herpes Simplex Virus 1 (12) and Human
72 Cytomegalovirus (8). We recently reported a similar finding with Kaposi's sarcoma-
73 associated herpesvirus (KSHV) (6). We previously found that KSHV hijacks the function
74 of host caspases to prevent IFN-β induction when KSHV re-enters the replicative (lytic)
75 cycle from a dormant (latent) infection state (20). Adding a small molecule caspase
76 inhibitor restores activation of the cytoplasmic DNA-sensing PRR cyclic GMP-AMP
77 synthase (cGAS) (6) and results in IFN-β induction (20). The amount of IFN-β produced
78 under these conditions based on ELISA measurements was substantial (20).
79 Nonetheless, subsequent scRNA-seq experiments revealed that the IFN-β comes from
80 a small population of cells, with less than 4% of infected cells producing it even under
81 this "derepressed" condition (6). The limited number of type I/III IFN producing cells
82 across a range of infections and cell types indicate that this is a feature of the IFN
83 induction system.

84 Since subversion of type I IFN is a key evolutionary tactic for viruses in the virus-
85 host arms race, heterogeneity in the expression and activity of IFN-inhibiting viral
86 proteins has been proposed as the reason for heterogeneous IFN-β expression (15,
87 20). However, we and others have found that viral gene expression heterogeneity does
88 not fully explain the observed IFN-β heterogeneity during infection with a range of
89 different viruses – KSHV, Influenza A Virus, Sendai Virus, and Newcastle Disease Virus
90 (6, 11, 19, 21, 22). In our scRNA-seq experiments with KSHV, IFN-β was only detected
91 in cells in the early stages of the KSHV lytic cycle, which made up 46% of the
92 population, indeed suggesting a contribution from viral regulation of IFN (6). Cells that
93 are latently infected with KSHV likely do not detect the infection, while cells in later lytic

94 viral stages have likely shut down host defenses effectively. However, only 6% of the
95 cells in the early lytic stages expressed IFN-β, demonstrating that viral replication stage
96 does not completely determine IFN induction (6). Moreover, when we compared IFN-β
97 positive and negative cells within this population, we did not find any viral gene that was
98 specifically missing in IFN-β-producing cells, as would be expected for a
99 heterogeneously expressed viral IFN suppressor (6). These findings suggested that
100 there is an additional, likely cellular, source of IFN-induction heterogeneity in this
101 system, that would explain the consistency of this phenomenon in other viral infections.
102 The host may benefit from limiting the percentage of cells producing IFN-β in an
103 infected population, as this may allow for optimal distribution of the cytokine and
104 protection of surrounding cells without IFNs reaching dangerous levels. However, how
105 IFN induction is restricted to a few cells remains unclear.

106 A potential mechanism could be restricted activation of one of the many signaling
107 steps that are needed for type I and III IFN transcriptional activation downstream of
108 PRRs. While different PRRs rely on different signaling adaptors, their signaling
109 pathways generally converge on the kinase TANK-binding kinase 1 (TBK1), which
110 phosphorylates the key transcription factor interferon regulatory factor 3 (IRF3). While
111 IRF3 activation is commonly used as the main indicator for IFN-β transcription triggered
112 by viral infection, IFN-β transcription also requires additional transcription factor
113 complexes, which together with IRF3 make up the IFN-β enhanceosome: the nuclear
114 factor kappa-light-chain-enhancer of activated B-cells (NF-κB) and the activator protein
115 1 (AP-1) complexes (23). Previous studies addressing IFN induction heterogeneity have
116 proposed different explanations on how this pathway may result in heterogeneity. Some

117 studies have suggested that promoter firing is inherently stochastic, so that all the
118 components including the transcription factors are active, but promoter firing only
119 happens in some cells (19, 24). One study suggested this was due to differences in the
120 3D structure of the genome (24), while another was unable to pinpoint the source of the
121 noise and concluded it may have to do with enhanceosome assembly (19). In contrast,
122 Zhao et al. proposed that every step leading to IFN induction is subject to
123 heterogeneous noise, from viral replication to signaling protein activation to abundance
124 of transcription factors (21). However, Zhao et al. did not control for the fact that many
125 genes encoding proteins in the IFN induction pathways are themselves ISGs, and also
126 used murine cells which do not require NF-κB for IFN induction (21). Overall, the cellular
127 source of the IFN induction heterogeneity remains poorly defined.

128 In this study, we used the KSHV lytic infection and caspase inhibition system to
129 further probe the source of heterogeneous IFN-β induction, as it provides robust and
130 sustained induction of IFN in the context of a viral infection. We developed a reporter
131 that allows us to separate cells expressing high vs. low levels of IFN-β and found that
132 surprisingly, the canonical IFN induction pathway culminating in IRF3 activation was
133 activated equally in both populations. However, activation or levels of other components
134 of the IFN-β enhanceosome better correlated with IFN-β induction. Thus, in our system,
135 activation of the NF-κB component RelA and baseline levels of the AP-1 component
136 ATF2 may be the limiting factors for IFN-β transcription at the single cell level.
137 Moreover, these findings suggest that that IRF3 serves as the infection signal, while AP-
138 1 and NF-κB provide the barrier to excessive IFN-β, at least in reactivating KSHV-
139 infected BC-3 cells. This study highlights the nuanced mechanics behind the induction

140 of a key component of our body's antiviral response and identifies specific cellular
141 factors that may contribute to limiting IFN-β induction to a small subpopulation of cells
142 during KSHV infection.
143

144 **Results**

145 *A fluorescent tdTomato reporter driven by a minimal human IFN-β promoter*
146 *distinguishes cells that express high vs. low levels of IFN-β*

147 Using scRNA-seq, we previously found that a very small fraction of KSHV-
148 infected cells produce IFN-β when the virus is reactivated and caspases are inhibited
149 (6). We calculated this fraction to be 3.8% of the total population and 6% of the infected
150 cells in the early stage of the lytic cycle. Nonetheless, the rare IFN-β producing cells
151 clustered together in our scRNA-seq data (6), suggesting that they have different
152 characteristics from other cell populations. To identify factors involved in IFN-β
153 regulation, we sought to separate and compare IFN-β producing and non-producing
154 cells. We previously engineered a tdTomato reporter driven by two copies of the 303 bp
155 minimal promoter sequence from the human *IFNB1* gene (Fig. 1A) and created stable
156 cell lines with this reporter in BC-3 cells (BC3-IFN-βp-tdTomato cells) (6). BC-3 cells are
157 latently KSHV-infected B cells isolated from a patient with primary effusion lymphoma
158 (25). The design of the promoter was based on previous reporters that used two copies
159 of the minimal IFN-β promoter sequence followed by luciferase or chloramphenicol
160 acetyltransferase (26-28). tdTomato was selected because it is the brightest fluorescent
161 protein whose signal is well separated from autofluorescence, which appears in the
162 green channel and is high in BC-3 cells (25, 29, 30). While our original scRNA-seq
163 study was performed in KSHV-infected epithelial cells, the iSLK.219 system (6), we

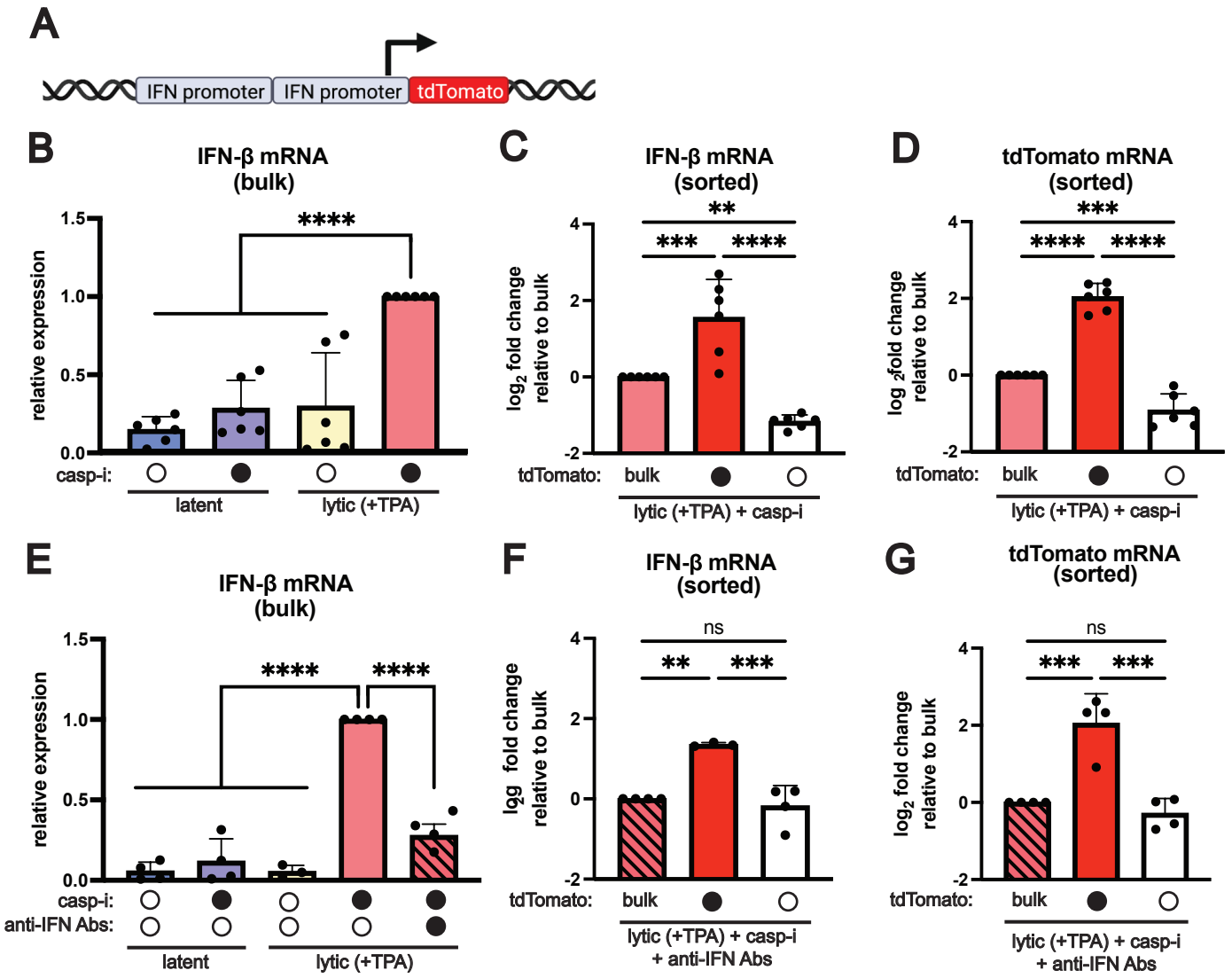

Figure 1. An IFN-β-promoter driven fluorescent reporter allows isolation of cells expressing high and low levels of IFN-β. A. Diagram of the IFN-βp-tdTomato reporter. Two copies of the 303 bp minimal promoter sequence for the human IFNB1 gene were cloned in front of the tdTomato fluorophore. This cassette was then introduced in BC-3 cells via lentiviral transduction for stable integration. **B-G**. BC3-IFN-β p-tdTomato reporter cells were treated with 20 ng/mL TPA for 48 hours to induce the lytic cycle ("lytic (+TPA)"). Where indicated, the cells were also treated with 10 μM of the pan-caspase inhibitor IDN-6556 ("casp-i") and/or with a cocktail of antibodies against type I IFNs and their receptor ("anti-IFN Abs") at 1:2000 dilution. IFN-β and tdTomato mRNA levels were measured by RT-qPCR and normalized to 18S rRNA. For **B** and **E**, IFN-β mRNA levels are normalized to the lytic+casp-i sample. For **C, D, F,** and **G**, the lytic+casp-i (**C, D**) or the lytic+casp-i+anti-IFN Ab (**F, G**) samples were sorted based on tdTomato expression and the fold enrichment in IFN-β and tdTomato RNA levels compared to unsorted ("bulk") samples is plotted in log2 scale. ns = p>0.05, ** = p<0.01, *** = p<0.001, **** = p<0.0001. One-Way ANOVA followed by Dunnett's (B, E) or Tukey's (C, D, F, G) post hoc multiple comparisons test. n=6 for B-D. n=4 for E-G.

164 chose BC-3s for subsequent experiments because they are more biologically relevant,
165 as B cells but not epithelial cells are the target of long-term KSHV infection in patients.
166 Moreover, the virus in iSLK.219 cells expresses GFP and RFP fluorescent reporters
167 (31), which restricts our options for fluorescent markers. In BC-3 cells, the KSHV lytic
168 cycle can be reactivated using the protein kinase C activator TPA. As we previously
169 reported (6), treating BC3-IFN-βp-tdTomato reporter cells with TPA and the pan-
170 caspase inhibitor IDN-6556 induced IFN-β compared to no treatment, TPA alone, or the
171 caspase inhibitor alone (Fig. 1B). Also, as we previously reported (6), only about 2% of
172 BC3-IFN-βp-tdTomato reporter cells expressed tdTomato (data not shown). TPA-
173 mediated reactivation is the most commonly used method of reliably reactivating KSHV
174 in primary effusion lymphoma cell lines such as BC-3 cells (32). However, TPA can
175 drive activation of multiple signaling pathways involved in growth, apoptosis, and
176 differentiation in different cell types through activation of protein kinase C (33, 34).
177 Therefore, to ensure that the use of TPA did not confound our studies, we measured
178 IFN induction in an uninfected EBV and KSHV-negative B cell lymphoma line, BJAB
179 cells, treated with TPA and the pan-caspase inhibitor IDN-6556 (35, 36). BJAB cells are
180 commonly used as an uninfected control for experiments with BC3 cells and other
181 primary effusion lymphoma cell lines (37, 38). We found that neither IFN-β nor the type
182 III IFN IFN-λ1 were induced after TPA and IDN-6556 treatment in uninfected BJAB cells
183 (Fig. 2). Therefore, we concluded that the IFN induction in BC-3 cells was indeed due to
184 KSHV lytic reactivation and virus sensing, not TPA addition, and that this system could
185 be used for further experiments.

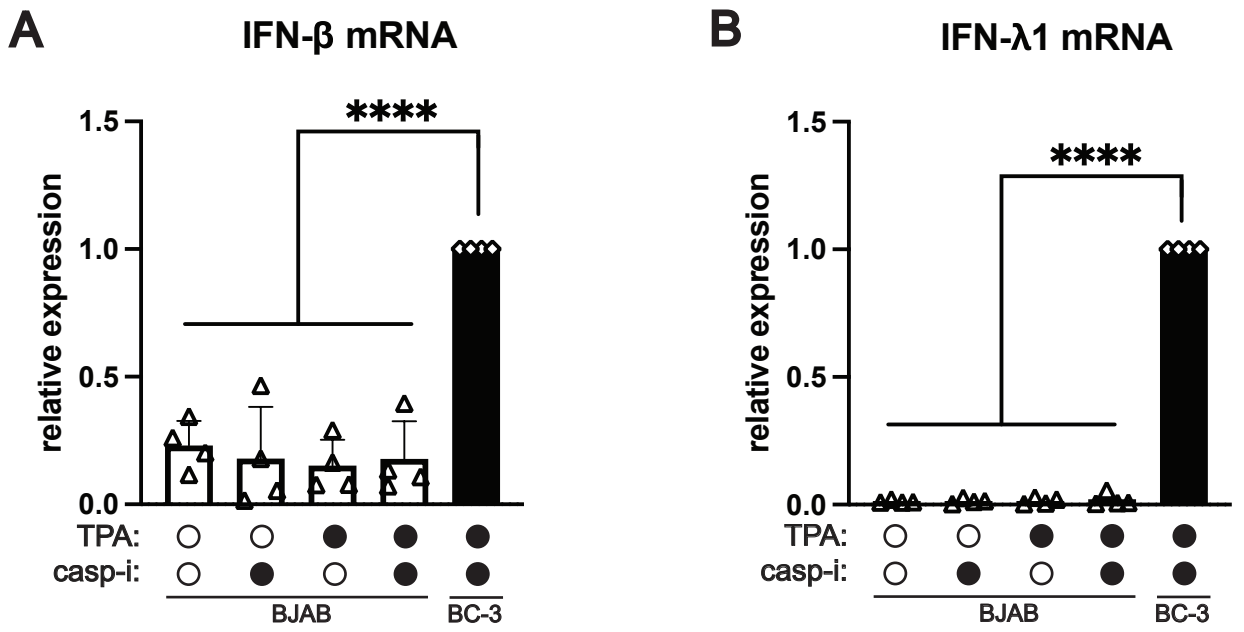

Figure 2. Treatment with TPA and caspase inhibitors does not induce IFN signaling in uninfected B cells. KSHV-negative BJAB cells were treated with 20 ng/ml TPA and/or 10 μM of the pan-caspase inhibitor IDN-6556 ("casp-i") for 48 hrs. BC-3 cells treated with TPA and IDN-6556 were used as a positive control for induction of type I and III IFNs. IFN-β (**A**) and IFN-λ1 (**B**) mRNA levels were measured by qRT-PCR and normalized to 18S rRNA. The expression levels are normalized to the TPA and IDN-6556-treated BC-3 sample for each experiment. **** = $p<0.0001$, One-Way ANOVA followed by Dunnett's post hoc multiple comparisons test. n=4.

186 To isolate cells expressing high and low IFN-β levels, we subjected the lytically
187 reactivated BC3-IFN-βp-tdTomato reporter cells treated with caspase inhibitors to
188 fluorescence-activated cell sorting (FACS) and collected tdTomato-positive and
189 negative cells. To confirm that tdTomato-based FACS results in separation of cells
190 based on IFN-β expression status, we measured tdTomato and IFN-β RNA levels in the
191 sorted samples. Importantly, we found that the endogenous IFN-β transcript was
192 enriched in the tdTomato+ cells and depleted in the tdTomato- cells, as was tdTomato
193 mRNA (Fig. 1C, D). IFN-β signaling also induces its own transcription (i.e. it behaves
194 like an ISG) (39), and indeed we saw in the scRNA-seq experiment that blocking IFN
195 responses with an anti-IFN antibody cocktail reduced the number of IFN-β-positive cells
196 (6). This antibody cocktail thus can allow us to specifically analyze the “first responder”
197 cells in which IFN-β was induced by pathogen sensing. Consistent with the scRNA-seq
198 results, we still observed IFN-β induction in the lytic cells treated with caspase inhibitors
199 after antibody treatment, although it was decreased (Fig. 1E). FACS based on the
200 tdTomato reporter also successfully enriched the rare IFN-β producing cells under these
201 conditions (Fig. 1F). These results demonstrate that FACS of the BC3-IFN-βp-tdTomato
202 reporter line allows us to separate cells producing high and low levels of IFN-β within a
203 population.
204
205
206 *IFN-β is not stochastically induced*
207 Some groups have proposed that heterogeneous expression of IFN-β may be
208 generated by stochasticity of IFN-β promoter firing (19, 24). This model posits that the
209 signals and activated proteins needed for IFN-β induction are present in all infected

210 cells, but transcription of IFN-β only occurs stochastically in some cells. To test this
211 hypothesis, we took advantage of the fact that pathogen sensing often induces type III
212 IFNs like IFN-λ1 in addition to type I interferons. The signaling cascade and
213 transcription factors that regulate IFN-β and IFN-λ1 are largely the same (40), so any
214 heterogeneity in upstream signaling should affect their induction in a coordinated way
215 (Fig. 3A). However, since they have separate promoters and are located on different
216 chromosomes, stochastic noise in assembly of the transcription factors or other aspects
217 of promoter firing (19) would differentially affect them. Contrary to the stochasticity
218 model, our results suggested that IFN-β and IFN-λ1 were induced in the same cells. In
219 the previously published scRNA-seq results, IFN-λ1 was also induced in iSLK.219 cells
220 upon lytic reactivation and caspase inhibitor treatment, and in the same rare cell
221 populations that expressed IFN-β, indicating a shared regulation mechanism (6). We
222 have since performed further analysis of the scRNA-seq data and found that indeed
223 expression of IFN-λ1 and IFN-β was highly correlated at the single cell level. In fact, no
224 other transcript showed closer correlation. We also analyzed IFN-λ1 expression after
225 sorting BC3-IFN-βp-tdTomato cells. Like IFN-β, IFN-λ1 was induced in BC-3 lytic cells
226 treated with caspase inhibitors (Fig. 3B). Moreover, IFN-λ1 was enriched and depleted
227 in concert with IFN-β in the tdTomato positive and negative cells, respectively (Fig. 3C).
228 This result indicates that IFN-β and IFN-λ1 were expressed in the same subset of cells.
229 Because IFN-λ1 can be induced as an ISG (Fig. 3A), we repeated the experiments in
230 the presence of anti-IFN antibodies to block paracrine signaling and checked that the
231 correlation was not a response to IFN. The pattern of IFN-λ1 and IFN-β co-expression
232 was also observed in the absence of IFN responses (Fig. 3E). These results stand in

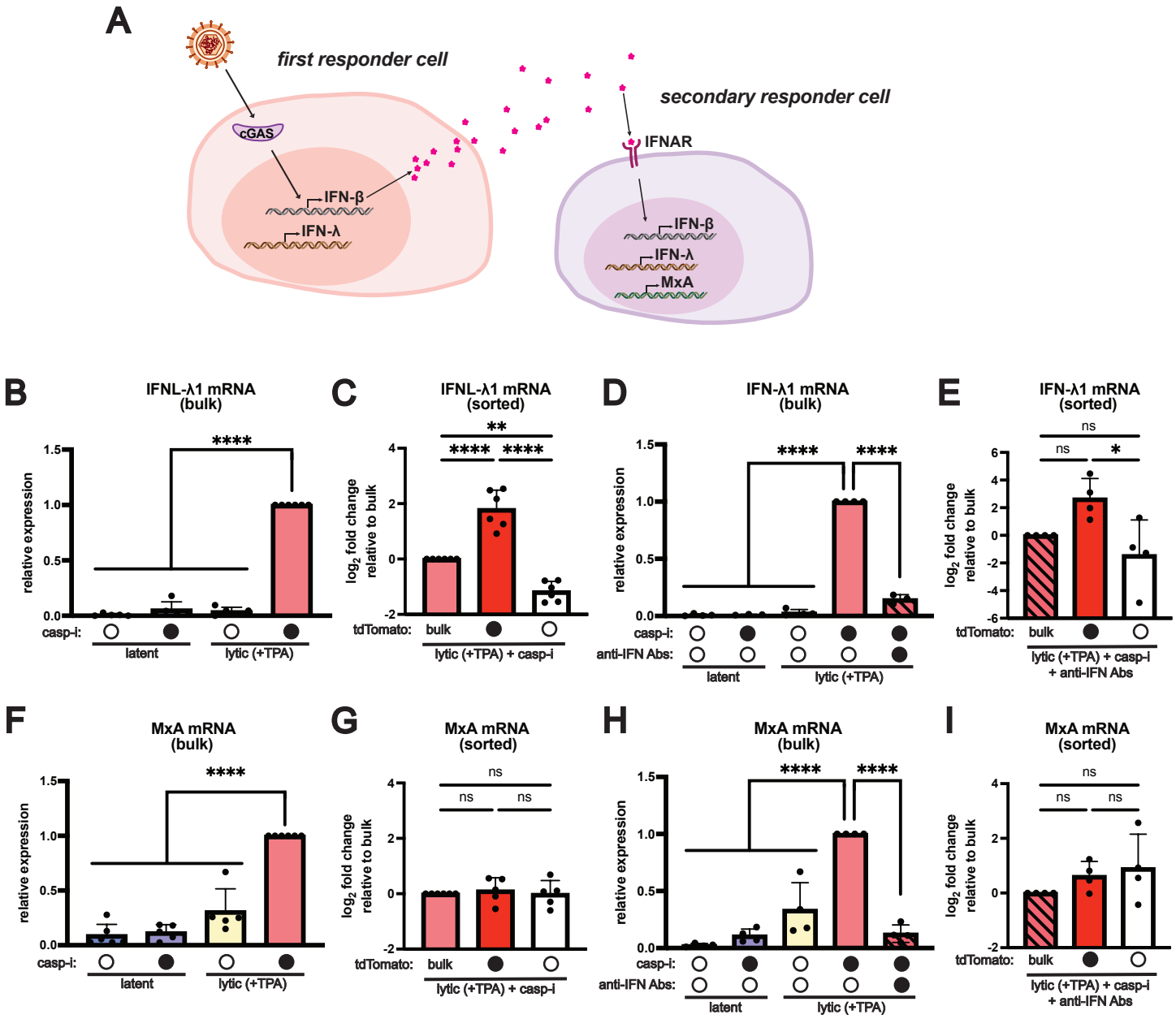

Figure 3. IFN-λ1 and IFN-β are coordinately induced in a subset of cells, pointing to heterogeneity in the induction pathway rather than stochastic noise in expression. A. Diagram of coordinate induction of IFN-β and IFN-λ. In first responder cells, IFN-β and IFN-λ are induced in response to infection or lytic reactivation downstream of PRRs, whereas in secondary responder cells, IFNs and ISGs such as MxA are induced in response to signaling downstream of IFN receptors. **B-I.** BC3-IFN-βp-tdTomato reporter cells were treated with 20 ng/ml TPA for 48 hours to induce the lytic cycle ("lytic (+TPA)"). Where indicated, the cells were also treated with 10 μM of the pan-caspase inhibitor IDN-6556 ("casp-i") and/or a cocktail of antibodies against type I IFNs and their receptor ("anti-IFN Abs") at 1:2000 dilution. IFN-λ1 (**B-E**) and MxA (**F-I**) mRNA levels were measured by RT-qPCR and normalized to 18S rRNA. In **B**, **D**, **F**, and **H**, IFN-λ1 and MxA mRNA levels are plotted relative to the lytic+casp-i sample. In **C**, **E**, **G**, and **I**, the lytic+casp-i (C, G) or the lytic+casp-i+anti-IFN Abs (E, I) samples were sorted based on tdTomato expression and the fold enrichment in IFN-λ1 (**C**) and MxA (**G**) mRNA levels compared to unsorted ("bulk") samples are plotted in log2 scale. ns = p>0.05, * = p<0.05, ** = p<0.01, **** = p<0.0001, One-Way ANOVA followed by Dunnett's (A, C, E, G) or Tukey's (B, D, F, H) post hoc multiple comparisons test. n=6 for A, B, E, F. n=4 for C, D, G, H.

233 contrast to MxA, an ISG that is induced in the lytically reactivated and caspase inhibitor-
234 treated cells in response to IFN signaling (Fig. 3A, F, H). Unlike IFN-λ1, MxA is not
235 enriched in sorted cells in the presence or absence of paracrine signaling,
236 demonstrating that the coordinate expression of IFN-λ1 and IFN-β was not related to
237 IFN-λ1 activation as an ISG (Fig. 3G, I). Moreover, anti-IFN antibodies block MxA
238 induction (Fig. 3H), confirming that the treatment blocks IFN responses as expected.
239 These results are consistent with the scRNA-seq data in iSLK.219 cells, where we
240 detected IFN-induced ISG expression in all cell clusters, not just the ones producing
241 IFN-β, whereas IFN-λ1 was mostly detected in IFN-β-producing clusters (6). Therefore,
242 we conclude that IFN-β and IFN-λ1 are not stochastically transcribed but coordinately
243 regulated. Moreover, the fact that they are expressed in the same rare subset of KSHV-
244 infected cells suggests that heterogeneity in the same upstream determinants leads to
245 cell-to-cell differences in type I and III IFN induction.
246
247 *TBK1 and IRF3 activity does not explain IFN-β heterogeneity*
248 The results above suggested that activation of the IFN-β induction pathway,
249 rather than IFN-β transcription, was heterogeneous. However, there are several
250 signaling steps in the IFN-β induction pathway that could be the bottleneck determining
251 whether cells transcribe IFN-β. Therefore, we monitored activation of the IFN-β
252 induction pathway, particularly the later steps of kinase and transcription factor
253 activation. Using inhibitors for cGAS and TBK1, we confirmed IFN-β induction is driven
254 by the cGAS-STING pathway through the TBK1 kinase in KSHV-reactivating B cells
255 (Fig. 4A), similarly to what we had previously found in the epithelial iSLK.219 cells (6,

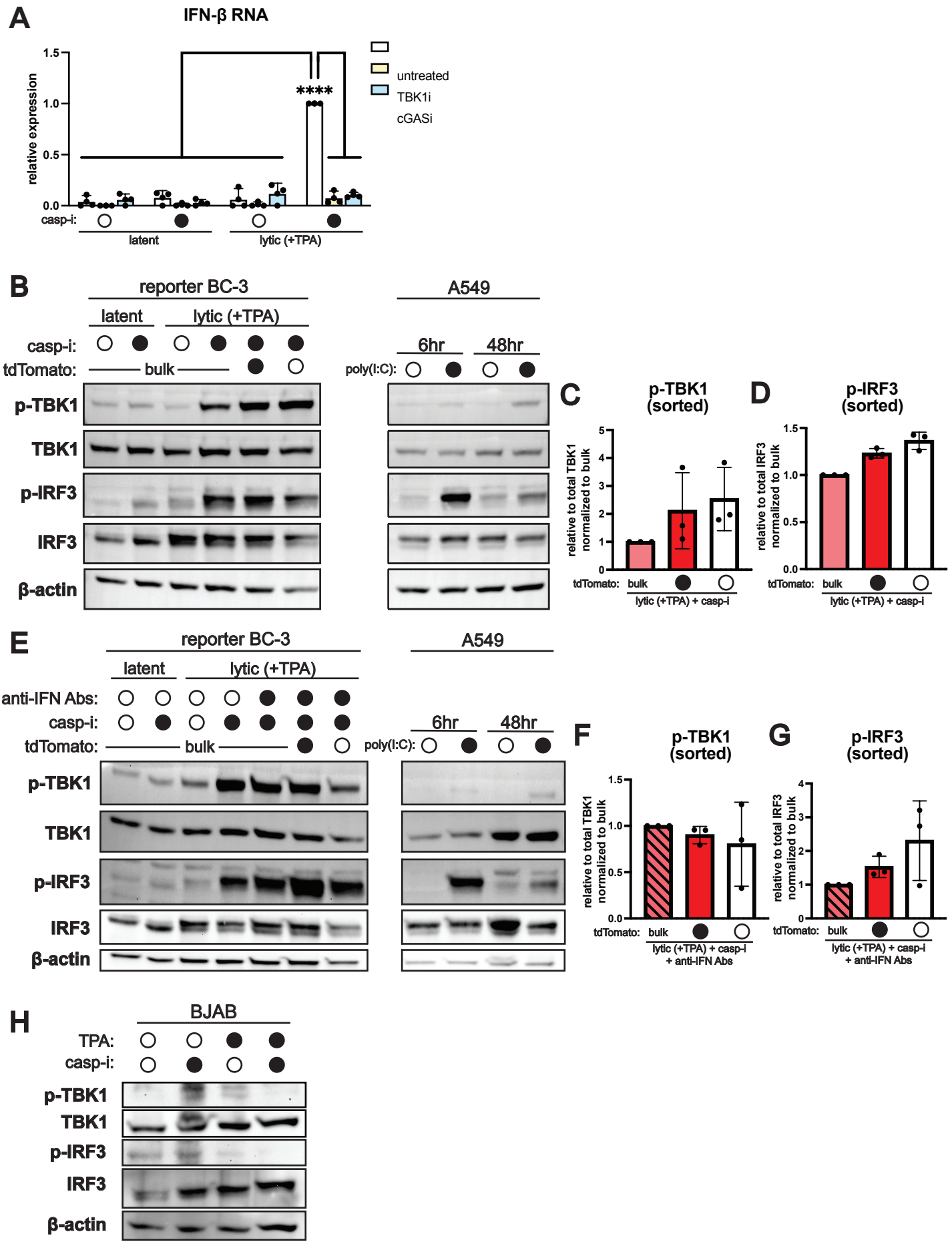
A
IFN-β RNA
relative expression
1.5
1.0
0.5
0.0
****
untreated
TBK1i
cGASi
casp-i:
latent
lytic (+TPA)
B
reporter BC-3
A549
latent
lytic (+TPA)
casp-i:
tdTomato:
bulk
6hr
48hr
poly(I:C):
p-TBK1
TBK1
p-IRF3
IRF3
β-actin
C
p-TBK1 (sorted)
relative to total TBK1 normalized to bulk
tdTomato:
bulk
lytic (+TPA) + casp-i
D
p-IRF3 (sorted)
relative to total IRF3 normalized to bulk
E
anti-IFN Abs:
F
G
lytic (+TPA) + casp-i + anti-IFN Abs
H
BJAB
TPA:

Figure 4. TBK1 and IRF3 are necessary but not sufficient to direct IFN-β expression, as they are activated even in cells with low IFN-β expression. BC3-IFN-βp-tdTomato reporter cells were treated with 20 ng/ml TPA for 48 hours to induce the lytic cycle ("lytic (+TPA)"). Where indicated, the cells were also treated with 10 μM of the pan-caspase inhibitor IDN-6556 ("casp-i"), 10 μM of the TBK1 inhibitor MRT76307 ("TBK1i"), 10 μM of the cGAS inhibitor G140 ("cGASi"), and/or a cocktail of antibodies against type I IFNs and their receptor ("anti-IFN Abs") at 1:2000 dilution. **A.** IFN-β mRNA levels were measured by qRT-PCR and normalized to 18S rRNA. The expression levels are normalized to "untreated" lytic+casp-i samples that did not receive TBK1i or cGASi for each experiment. n=3. **** = $p<0.0001$. Two-Way ANOVA followed by Tukey's post hoc multiple comparisons test. **B-H.** Protein lysates were probed for phosphorylated IRF3 (Ser386), total IRF3, phosphorylated TBK1 (Ser172), total TBK1, and β-actin as a loading control. As a positive control for IRF3 and TBK1 activation/phosphorylation, A549 cells were treated with poly(I:C) for 6 and 48 hours before protein lysates were collected. Protein was isolated from treated BC3-IFN-βp-tdTomato reporter cells without sorting ("bulk"), or after sorting the ytic+casp-i (**B-D**) or lytic+casp-i+anti-IFN Abs (**E-H**) sample based on tdTomato expression. Western blot for phosphorylated TBK1 (**C**, **F**) and phosphorylated IRF3 (**D**, **G**) were quantified by normalizing the density of phosphorylated protein to unphosphorylated protein bands per lane for bulk lytic+casp-i treated samples and sorted tdTomato+ and tdTomato- samples.
H. KSHV-negative BJAB cells were treated with vehicle, 20 ng/ml TPA, and/or 10 μM of the pan-caspase inhibitor IDN-6556 ("casp-i") for 48 hours. Protein was isolated and stained for phosphorylated TBK1, total TBK1, phosphorylated IRF3, and total IRF3. Images shown are representative of 3 replicates (**B**, **E**) or 2 replicates (**H**).

256 20). We thus tested whether TBK1 was activated only in the cells that induced IFN-β by
257 comparing levels of phosphorylated TBK1 in lytically reactivated, caspase inhibitor-
258 treated cells sorted based on tdTomato status. To ensure the antibodies detected the
259 correct bands, we used poly(I:C)-treated A549 cells as positive controls for TBK1
260 phosphorylation. In every experiment, tdTomato-based sorting resulted in the expected
261 enrichment and depletion of IFN-β mRNA in tdTomato+ and tdTomato- cells,
262 respectively (RNA measurements are shown in Fig. 1C). However, surprisingly, we
263 observed no difference in activated (phosphorylated) TBK1 between IFN-β high and low
264 cells (Fig. 4B, C). Since TBK1 phosphorylates and activates the well-characterized IFN-
265 β transcription factor IRF3, we also tested whether IRF3 was differentially activated in
266 the IFN-β high vs. low cells (i.e. tdTomato+ and -), again using poly(I:C)-treated A549
267 cells as a positive staining control. Like TBK1, we observed no difference in IRF3
268 phosphorylation between the two populations (Fig. 4B, D). We also observed no
269 difference in TBK1 and IRF3 phosphorylation between IFN-β high and low cells when
270 we blocked autocrine and paracrine IFN-β signaling with anti-IFN antibodies (Fig. 4E-
271 G). Therefore, while both TBK1 and IRF3 were active in lytic cells treated with caspase
272 inhibitors, their activation alone was not predictive of IFN-β induction. To ensure that the
273 lytic cycle-inducing TPA treatment was not a confound for these experiments, we
274 treated uninfected BJAB cells with the same drugs (TPA and the caspase inhibitor IDN-
275 6556). We confirmed that these treatments did not activate TBK1 and IRF3 in the
276 absence of KSHV infection (Fig. 4H). These results indicate that the canonical IFN
277 induction pathway is activated in many, likely most, lytically reactivated KSHV-infected

278 BC-3 cells when caspases are inhibited. However, an additional factor besides IRF3
279 activation keeps IFN-β induction limited to a small fraction of the population.
280
281 *AP-1 expression and NF-κB activation correlate with IFN-β induction and may drive*
282 *heterogeneity*
283 IRF3 activation is assumed to lead to IFN-β transcription, and phosphorylation of
284 IRF3 is commonly used as a proxy for IFN induction. However, the IFN-β
285 enhanceosome contains two additional transcription factor complexes: AP-1 and NF-κB
286 (Fig. 5A) (41-43). While both the AP-1 and NF-κB complexes can be composed of many
287 different members depending on the context, AP-1 complexes formed by c-Jun and
288 ATF2 and NF-κB complexes formed by the RelA/p65 and NFKB1/p50 subunits have
289 been specifically linked to IFN-β transcription during viral infections (43). NF-κB and
290 IRF3 are also verified transcription factors for IFN-λ1 (44). How AP-1 and NF-κB are
291 activated during IFN-β induction and their relation to activation of cGAS and other PRRs
292 is not well understood. Given that IRF3 activation did not explain IFN-β heterogeneity,
293 we considered the possibility that AP-1 and/or NF-κB might be determinants of
294 heterogeneous IFN-β induction in our system. We previously reported that expression of
295 NF-κB family members were enriched in IFN-β-expressing cells based on single cell
296 RNA-seq analysis of KSHV-infected epithelial cells treated with caspase inhibitors (6).
297 We reanalyzed the scRNA-seq dataset to test whether this was also the case for the
298 AP-1 components. To further explore the relationship between IFN-β and these
299 transcription factors, we separated the cells from the two IFN-β expressing clusters by
300 IFN-β status. The AP-1 component ATF2 was enriched in both IFN-β-positive and

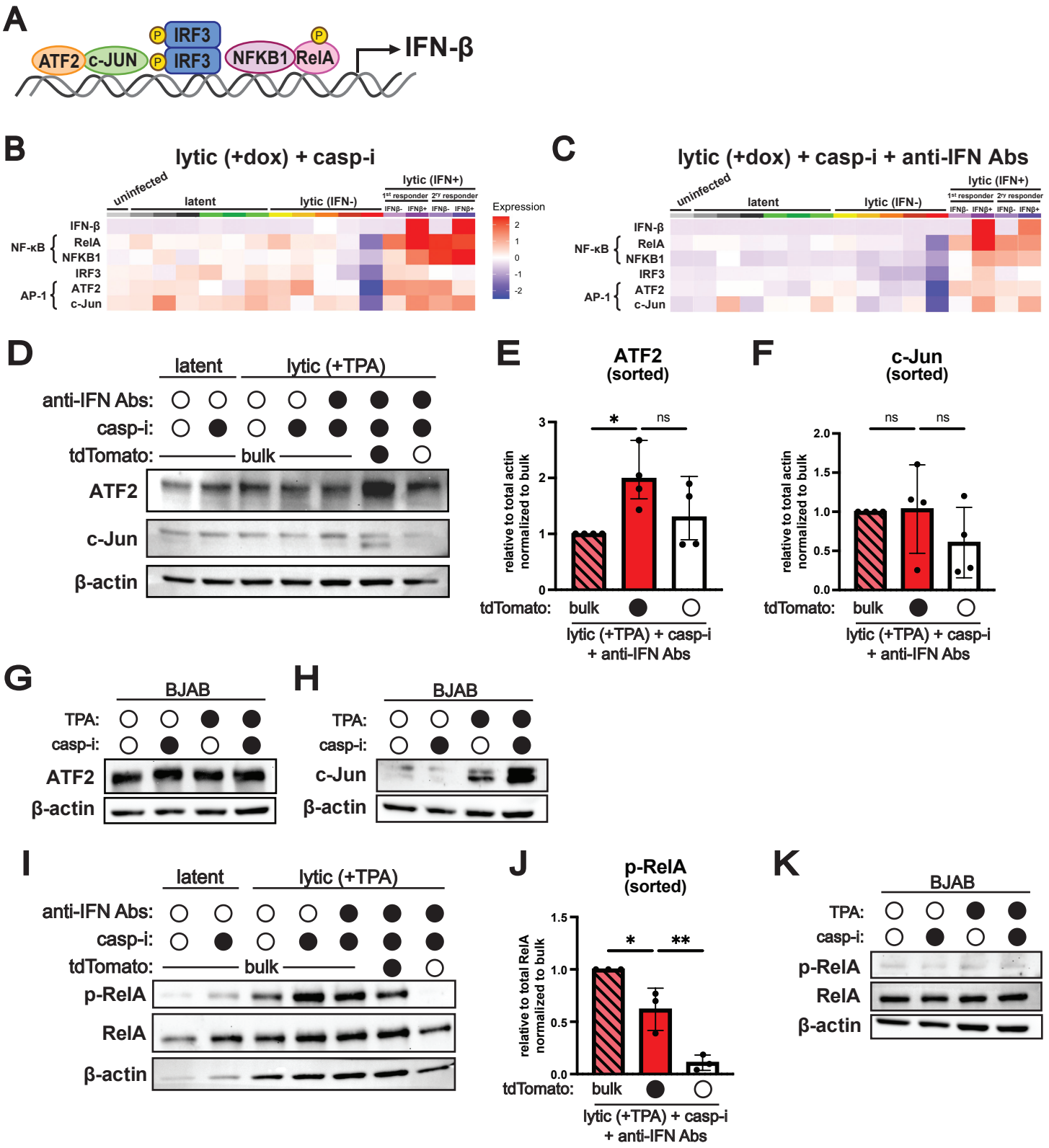
A
ATF2
c-JUN
IRF3
IRF3
NFKB1
RelA
IFN-β
B
lytic (+dox) + casp-i
uninfected
latent
lytic (IFN-)
lytic (IFN+)
1st responder
2ry responder
IFNβ-
IFNβ+
Expression
NF-κB
IFN-β
RelA
NFKB1
AP-1
IRF3
ATF2
c-Jun
C
lytic (+dox) + casp-i + anti-IFN Abs
D
latent
lytic (+TPA)
anti-IFN Abs:
casp-i:
tdTomato:
bulk
ATF2
c-Jun
β-actin
E
ATF2
(sorted)
relative to total actin normalized to bulk
ns
tdTomato:
bulk
lytic (+TPA) + casp-i
+ anti-IFN Abs
F
c-Jun
(sorted)
G
BJAB
TPA:
casp-i:
ATF2
β-actin
H
c-Jun
I
p-RelA
RelA
J
p-RelA
(sorted)
K

Figure 5. Levels of the AP-1 subunit ATF2 and phosphorylation of the NF-κB subunit RelA are higher in cells with high IFN-β expression. A. Diagram of the IFN-β enhanceosome and its position on the IFN-β promoter. In the IFN-β enhanceosome, NF-κB is composed of subunits NFKB1 (p50) and RelA, and AP-1 is composed of subunits ATF2 and c-Jun. **B-C**. Re-analysis of single-cell RNA sequencing (scRNA-seq) data in Tabtieng, Lent, et al 2022. iSLK.219 cells were treated with 1 μg/mL doxycycline for 4 days to induce the lytic cycle ("lytic"). The cells were also treated with 10 μM of the pan-caspase inhibitor IDN-6556 ("casp-i"), as well as a mixture of antibodies against type I IFNs and its receptor ("anti-IFN Abs") (**C** only) to block IFN-β paracrine signaling. The average mRNA levels of genes in the IFN-β enhanceosome from the scRNA-seq data are shown for each of the 12 clusters of cells identified by the original analysis (indicated by different colors above the heatmap). Clusters were classified as "lytic" or "latent" based on the pattern of viral genes they expressed. The "lytic IFN-β-positive" clusters were further separated into two groups based on the IFN-β status of individual cells. **D-F, I-J**. BC3-IFN-βp-tdTomato reporter cells were treated with 20 ng/ml TPA for 48 hours to induce the lytic cycle ("lytic (+TPA)"), 10 μM of the pan-caspase inhibitor IDN-6556 ("casp-i"), and/or a cocktail of antibodies against type I IFNs and their receptor ("anti-IFN Abs") to block IFN-β paracrine signaling. Protein was isolated from BC3-IFN-βp-tdTomato reporter cells without sorting ("bulk"), or after sorting the lytic+casp-i+anti-IFN Abs based on tdTomato expression. Western blots were probed for ATF2, c-Jun (**D**), or total RelA and phosphorylated RelA (Ser536) (**I**) or β-actin as a loading control. Levels of ATF2 (**E**) and c-Jun (**F**) in sorted samples were quantified from the western blots, normalized to β-actin, and plotted relative to bulk lytic+casp-i+ anti-IFN Abs samples. Levels of phosphorylated RelA (Ser536) (**J**) were quantified by normalizing to total RelA and plotted relative to bulk lytic+-casp-i+ anti-IFN Abs samples. **G, H, K**. KSHV-negative BJAB cells were treated with vehicle, 20 ng/ml TPA and/or 10 μM of the pan-caspase inhibitor IDN-6556 ("casp-i") for 48 hrs. Protein was isolated and stained for ATF2 (**G**), c-Jun (**H**), phosphorylated (Ser536) and total RelA (**K**), and β-actin as a loading control. Images are representative of 4 replicates (**D**), 3 replicates (**I**), or 2 replicates (**G, H, K**). ns = $p>0.05$, * = $p<0.05$, ** = $p<0.01$, One-Way ANOVA followed by Tukey's post hoc multiple comparisons test.

301 negative cells within the IFN-β expressing clusters, while the AP-1 component c-Jun
302 and the NF-κB components RelA and NFKB1 were specifically enriched in the IFN-β-
303 positive cells (Fig. 5B). These enrichments were particularly evident when anti-IFN
304 blocking antibodies were added to prevent paracrine and autocrine signaling, because
305 most of these genes were also induced by IFN-β signaling (Fig. 5C). To note, there was
306 an enrichment of IRF3 mRNA in the IFN-β-producing cells in the scRNA-seq data (Fig.
307 5B-C), even though we did not detect enrichment at the protein level in BC-3 cells (Fig.
308 4B, E). We also observed that after blocking paracrine signaling, IFN-β expression was
309 reduced in one of the IFN-β expressing clusters (Fig. 5B-C). This cluster may represent
310 "secondary responder" cells that express IFN-β as an ISG, while the other cluster may
311 comprise "first responder" IFN-β-producing cells. These results are consistent with the
312 overall reduction in IFN-β induction that we saw upon addition of the anti-IFN antibodies
313 (Fig. 1E).

314 We then tested whether NF-κB and AP-1 were similarly enriched at the protein
315 level in BC-3 cells expressing high levels of IFN-β. To reduce confounds from paracrine
316 signaling observed in the scRNA-seq results, we performed the FACS experiments with
317 anti-IFN blocking antibodies. Interestingly, we observed an enrichment in the AP-1
318 component ATF2 in tdTomato+ cells, indicating that ATF2 levels are higher in cells that
319 express high levels of IFN-β (Fig. 5D, E). Total ATF2 levels did not change between
320 conditions in bulk samples, indicating that ATF2 expression was not induced during
321 infection and/or by caspase inhibitor treatment. Instead, these results suggest that basal
322 expression of ATF2 is variable and that IFN-producing cells had higher ATF2 levels
323 prior to lytic reactivation (Fig. 5D). Levels of the other AP-1 component, c-Jun, were

324 variable across replicates, but in two out of three replicates a unique shorter isoform
325 was detected in the sorted IFN-β high cells (Fig. 5D). However, this shorter c-Jun
326 isoform was also induced by treatment of uninfected BJAB cells treated with TPA and
327 caspase inhibitors, suggesting that its appearance may be unrelated to viral replication
328 and IFN induction (Fig. 5H), as IFN-β is not induced in uninfected cells (Fig. 2). ATF2
329 levels were not changed by TPA and/or caspase inhibitor treatment in uninfected BJAB
330 cells. In addition, we also found that IFN-β high cells are enriched in phosphorylated
331 RelA, one of the NF-κB components, whereas there was little to no phosphorylated
332 RelA in the IFN-β low cells (Fig. 5I-J). This result points to RelA activation only in IFN-β
333 high cells. RelA phosphorylation was not increased by TPA and/or caspase inhibitor
334 treatment in uninfected BJAB cells, indicating this was specific to infected cells (Fig.
335 5K). Overall, these results indicate that ATF2 and p-RelA likely have important roles in
336 cell-specific IFN-β induction. Particularly elevated ATF2 levels may be needed for IFN-β
337 induction, while RelA is likely activated in response to a stimulus but may serve to
338 potentiate IFN transcription in the small subset of IFN producing cells (Fig. 6).
339

340 **Discussion**

341 In this study, we investigated underlying differences between cells that induce
342 high vs. low levels of IFN-β in the context of KSHV infection and caspase inhibition. We
343 reveal that the IFN-β enhanceosome components AP-1 and NF-κB, but not IRF3, are
344 likely to determine whether individual cells induce IFN-β during KSHV and caspase
345 inhibition. Protein levels of the AP-1 factor ATF2 and phosphorylation of the NF-κB
346 factor RelA were higher in cells that express high levels of IFN-β than in cells that
347 express minimal IFN-β. ATF2 levels were not upregulated under IFN-inducing

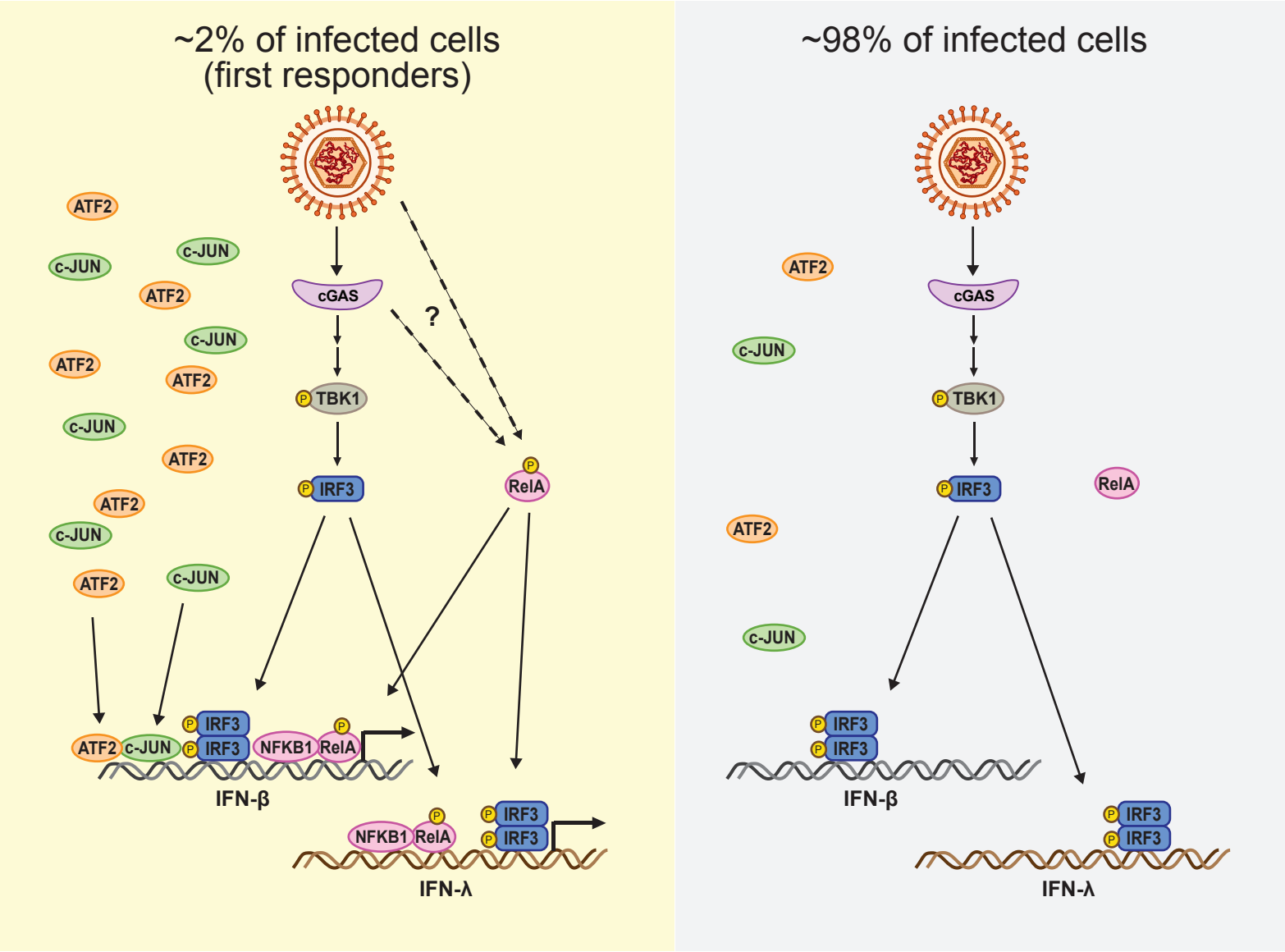

Figure 6. Model of regulation of heterogeneous IFN-β expression by components of the IFN-β enhanceosome. (Left) In the rare cells that induce IFN-β during viral infection as “first responders”, there are high levels of the AP-1 factor ATF2 and both the NF-κB subunit RelA and IRF3 become phosphorylated in response to infection. This results in the formation of the IFN-β enhanceosome and in IFN-β and IFN-λ1 transcription. (Right) In the majority of virally infected cells, there are lower amounts of ATF2, and RelA is not phosphorylated during infection. While IRF3 is still activated, the full IFN-β enhanceosome does not form and IFN-β and IFN-λ1 are not induced.

348 conditions in bulk samples, suggesting that sorting for cells with high IFN-β enriched for
349 cells with high ATF2. Therefore, this result points to a model whereby ATF2
350 heterogeneity precedes viral reactivation and only cells with higher ATF2 are able to
351 respond to pathogen cues by turning on IFN-β. In contrast, RelA was only activated
352 under IFN-inducing conditions, which suggests a possible bottleneck to its activation in
353 most cells. Our findings thus support a model in which IFN-β inducibility during KSHV
354 lytic replication is limited to a rare fraction of cells with elevated baseline ATF2 levels
355 and activated NF-κB. While IRF3, AP-1, and NF-κB have long been known to regulate
356 IFN transcription, the cell-to-cell heterogeneity in their levels and activation has not
357 previously been reported. Moreover, this is the first description of the unique role of AP-
358 1 and NF-κB in possibly controlling which individual cells make IFN, despite cGAS-to-
359 IRF3 signaling being on in almost all cells in the population.

360 Host regulation of IFN-β is important given its potent effects on both the host and
361 pathogen through autocrine and paracrine induction of hundreds of ISGs. Insufficient
362 induction of ISGs can lead to susceptibility to infection, while excessive IFN-related
363 inflammation can lead to autoimmune disorders and excessive tissue damage. A
364 system in which the barrier for IFN-β induction is very high may provide an appropriate
365 level of innate immune alarm by limiting IFN-β expression to a small fraction of infected
366 cells. The fact that many viral infections display heterogeneous IFN induction in a way
367 that is not fully explained by viral factors (11, 19, 21, 22), in combination with our
368 results, suggests that an important part of the mechanism of IFN regulation is rooted in
369 cellular heterogeneity. Furthermore, heterogeneous expression of other cytokines such

370 as IL-2 (45), IL-4 (46, 47), IL-5 (48), and IL-10 (49) has been reported, suggesting this is
371 an important mode of immune regulation.

372 Interestingly, while IRF3 and TBK1 are required for IFN induction following
373 PAMP/DAMP signaling, here we found they are not sufficient for IFN-β induction.
374 Although IRF3 activation is often used as a proxy for IFN-β induction, especially in
375 studies of viral infections, our results indicate that this one-to-one relationship is not true
376 at the level of individual cells. Indeed, both TBK1 and IRF3 appear to be activated
377 regardless of the IFN-expressing status of the cells. Most likely, the upstream
378 components of the IFN induction pathway, including the PRR (cGAS in this case), are
379 also activated regardless of the IFN status of the cells. Instead, our results point to the
380 other IFN-β enhanceosome factors, AP-1 and NF-κB, as the potential limiting factors
381 that determine IFN-β induction in individual cells. We propose a model where activation
382 of IRF3 is the main signal that reports on the presence of an infection, while the main
383 function AP-1 and NF-κB is to provide an additional barrier to limit IFN-β induction to a
384 small subset of cells among an infected population.

385 The regulation of AP-1 and NF-κB during IFN responses is not as well
386 characterized as the activation of IRF3. For AP-1, our results suggest that differences
387 may precede infection, because at the bulk level there is no clear change in ATF2
388 levels. Therefore, the simplest interpretation for our results (Fig. 5D) is that some cells
389 have higher ATF2, and these cells are more abundant in the IFN-producing pool. We
390 were unable to detect changes in phosphorylation of ATF2 and c-Jun under IFN-
391 inducing conditions, suggesting this activation step may be dispensable (data not
392 shown). In contrast, NF-κB is likely activated in a subset of cells under IFN-inducing

393 conditions. While IRF3 and NF-κB may both be activated downstream of STING based
394 on previous studies (50, 51), the fact that NF-κB is only phosphorylated in IFN-β high
395 cells while IRF3 is also phosphorylated in IFN-β low cells indicates that there must be a
396 heterogenous bottleneck specifically for NF-κB activation. We attempted to use
397 inhibitors of the IκB kinases α and β (IKKα/β), which activate RelA under other
398 conditions (52-54), to test whether they are required for RelA phosphorylation and IFN-β
399 induction in KSHV infection. However, IKKα/β inhibitors strongly inhibited reactivation
400 (data not shown), which precluded testing of effects on IFN-β induction. We also tested
401 inhibitors of the transforming growth factor-β-activated kinase 1 (TAK1), which in many
402 signaling pathways is upstream of IKKα/β (55), but this inhibitor had no effect on IFN-β
403 levels or phosphorylation of RelA in our system (data not shown). Therefore, we still do
404 not know whether IKKα/β or other kinases phosphorylate NF-κB during IFN-β induction
405 in our system.

406 While this study has shed light on the expression mechanics of IFN-β during
407 KSHV infection, it is possible that the mechanism of IFN heterogeneity is different for
408 other viral infections and cell types. Although IFN heterogeneity is a widespread feature
409 of viral infection, reported by every study we have encountered, the PRRs and signaling
410 pathways that lead to IFN induction vary (6-18, 56). Moreover, IFN-β expression
411 patterns appear to differ between cell types. For example, a larger proportion of
412 dendritic cells express IFN-β upon infection (19, 57, 58) compared to other cell types
413 such as fibroblasts and epithelial cells (6-16). Flexibility in tailoring the IFN response to
414 factors such as cell type, viral load, and PAMP type is likely evolutionarily beneficial in

415 mounting an appropriate immune response. More studies identifying the determinants of
416 IFN expression are needed to parse out the ubiquity vs. uniqueness of our findings.
417 Although our findings suggest there is a high barrier to IFN-β induction, results
418 from studies using Sendai virus suggest that heterogeneity of IFN-β induction is not due
419 to a complete inability of some cells to induce IFN-β. Infection with a highly inflammatory
420 strain of Sendai virus (the Cantell strain) induced IFN-β expression in 99% of infected
421 A549 cells (11, 58). In comparison, only 0.48% of A549 cells expressed IFN-β during
422 infection with influenza A virus (11). This indicates that IFN-β regulation can be
423 overridden given excessive stimuli such as the defective-interfering viral genomes that
424 characterize the Sendai virus strain Cantell (59). These observations also suggest that
425 the strength or abundance of the stimulus may matter. Indeed, strong IFN inducers like
426 Newcastle Disease Virus, Sendai virus strain Cantell, or the potent PAMP mimetic
427 poly(I:C) induce IFN-β in a larger proportion of cells (10-99%) (21, 22, 56, 57, 60-63)
428 compared to other viral infections and treatments (1-10%) (6-17). Unfortunately, we
429 have been unable to test whether the relationship between stimulus strength and
430 percentage of IFN-expressing cells is also true in KSHV-reactivating BC-3 cells, as we
431 have not identified a stronger stimulus that worked in these cells. In order to isolate the
432 cells that express IFN-β, the cells need to be active and viable for long enough for the
433 tdTomato fluorescent protein to express and accumulate to detectable levels.
434 Commonly used IFN-inducing stimuli (poly(I:C), 2’3’-cGAMP, STING agonist diABZI,
435 TLR7 agonist imiquimod, and plasmid DNA) either did not induce IFN-β expression in
436 BC-3 cells or induced cell death before we could measure tdTomato production (data
437 not shown). IFN-β induction through KSHV reactivation and caspase inhibition allows for

438 sustained IFN-β induction without inducing cell death, which gives us a unique tool to
439 study the elusive phenomena of cellular heterogeneity in IFN-β induction.
440 While our scRNA-seq data did not reveal any correlations between viral genes
441 and IFN-β expression (6), technical limitations mean that we may have missed some
442 important component. For example, the scRNA-seq would not have captured mutations
443 in KSHV that may have risen in individual cells. Moreover, the sequencing method was
444 3' end directed, and many mRNAs in KSHV share 3' end sequences, preventing
445 accurate measurement of some viral genes. KSHV has evolved a large arsenal of
446 proteins that antagonize IFN signaling. KSHV ORF52 can prevent cGAS activation by
447 sequestering DNA substrates by phase separation mechanism (64), and a truncated
448 and therefore cytoplasmic form of KSHV LANA also inhibits cGAS (65). KSHV ORF33
449 aids in inactivating the cGAS-adaptor STING (66). One study found that the KSHV
450 homolog of human IRFs vIRF1 inhibits IFN-β by preventing STING and TBK1 activation
451 during KSHV reactivation in iSLK.219 cells (67). However, these viral factors all act
452 upstream of IRF3 activation, which is still active even in IFN-β-low cells in our system,
453 and are therefore unlikely to explain IFN induction heterogeneity. KSHV vIRFs have
454 also been implicated in regulating IFNs at the transcriptional level. Studies on KSHV
455 vIRF3 and vIRF4 have found that these inhibit IRF7, which is important for inducing
456 secondary responder cells (68, 69). A study on KSHV vIRF2 found that it induces IRF3
457 degradation via caspase-3 (70). Another study found KSHV vIRF1 inhibits IFNA4
458 induced by Newcastle Disease Virus in murine cells by preventing p300 from binding to
459 IRF1 and IRF3 (71). Similarly, another study found KSHV vIRF1 binds CBP/p300 to
460 prevent IRF3 complex formation on the IFN-β promoter during Sendai Virus infection in

461 293T cells (72). Potentially, these events could create a barrier downstream of IRF3
462 phosphorylation, but this remains to be tested. Also, there has been no reports of any
463 KSHV factor that regulates AP-1 levels or blocks NF-κB activation, so there is no
464 obvious viral explanation for the heterogeneity we observe for these factors.

465 There are some limitations to our study. First, our reporter system likely does not
466 fully recapitulate native IFN-β mRNA expression and kinetics. The minimal IFN-β
467 promoter lacks the native chromatin environment and potential long range promoter
468 elements. The reporter also lacks the native 3' untranslated region of the IFN-β mRNA,
469 which makes this mRNA unstable. Also, it is likely that only cells with sustained IFN-β
470 promoter activity were detected and sorted, as sufficient accumulation of the tdTomato
471 protein is needed for FACS. However, despite these imperfections, we were able to
472 successfully separate the cells that expressed high and low levels of IFN-β at the time
473 of sorting (Fig. 1C). Also, while our results point to cellular heterogeneity as a major
474 determinant of IFN-β regulation, we cannot completely rule out the possibility that the
475 heterogeneity of AP-1 and NF-κB is regulated by the virus, as described above. Lastly,
476 while TPA is a very effective inducer of lytic KSHV reactivation and is commonly used in
477 KSHV research (32), it is also a known inducer of NF-κB. This is a potentially
478 confounding variable. Our concerns are reduced by the fact that treatments that induce
479 IFN-β in infected BC-3 cells do not induce IFN-β or phosphorylation of TBK1, IRF3, or
480 RelA in the uninfected BJAB cells at comparable time points, indicating viral reactivation
481 rather than TPA treatment drives signaling changes in our system (Figs. 2, 4H, 5K).
482 Moreover, to date, all of our results are consistent between the BC-3 and iSLK.219

483 KSHV-infected cell lines, even though iSLK.219 cells are not treated with TPA to induce
484 the lytic cycle. This also suggests that our results are not simply due to TPA effects.
485 Despite the described limitations, this study points to a new model of
486 heterogeneous type I interferon transcription during viral infection as the result of
487 inherent cellular heterogeneity in protein levels and protein activation. More studies are
488 needed to pinpoint the earliest source of the heterogeneity and to examine the
489 mechanism of enrichment and activation of AP-1 and NF-κB in the context of antiviral
490 responses.
491
492 **Materials and Methods**
493
494 *Cell lines, reagents, and treatments*
495 All cells were cultured at 37°C and 5% CO_2. HEK293T cells were grown in Dulbecco's
496 modified Eagle's medium (DMEM; Life Technologies) supplemented with 10% fetal
497 bovine serum (FBS; Hyclone). BC-3 cells and derivatives were maintained at a density
498 of $5x10^5$ cells/mL in Roswell Park Memorial Institute medium (RPMI; Life Technologies)
499 supplemented with 20% FBS, 2 mM GlutaMAX (Gibco), and 55 μM β-mercaptoethanol
500 (BME; Gibco). BC-3-IFN-βp-tdTomato cells were generated as described in Lent,
501 Tabtieng, et al., 2022 (6). For reactivation, BC-3 and BC-3-IFN-βp-tdTomato cells were
502 seeded at a density of $5x10^5$ cells/mL and treated with 20 ng/mL TPA (12-O-
503 tetradecanoylphorbol-13-acetate; MilliporeSigma 5244001MG) in dimethylsulfoxide
504 (DMSO; Sigma Aldrich Fine Chemicals Biosciences). Reactivation was measured in all
505 experiments, ranged between 20% and 60%, and was not significantly different in any

506 of the conditions tested. Where indicated, cells were treated with vehicle (DMSO), 10
507 μM IDN-6556 (Emricasan; Selleck Chemical LLC S777525MG), a mixture of
508 neutralizing antibodies against type I IFNs at 1:2000 dilution (PBL Assay Science
509 39000-1), 10 μM TBK1 inhibitor (MRT67307; Medchemexpress LLC HY130185MG),
510 and/or 10 μM cGAS inhibitor (G140; Invivogen inh-g140).
511
512 *Fluorescence-activated cell sorting*
513 100 mL of BC-3-IFN-βp-tdTomato cells were seeded at a density of $5x10^5$ cells/mL and
514 treated with TPA, IDN-1665, and, where indicated, an anti-IFN antibody mixture as
515 described above. After two days, they were collected and stained with 1 μg/mL DAPI
516 (4',6-Diamidino-2-Phenylindole, Dihydrochloride) stain (Invitrogen, D1306) for 5 minutes
517 at room temperature. They were then washed in PBS and filtered through a 35 μm
518 strainer (Chemglass Life Sciences CLS4380009) and sorted based on tdTomato
519 fluorescence on a BD FACSAria III at the University of Wisconsin Carbone Cancer
520 Center Flow Cytometry Laboratory core facility. The DAPI stain was used to remove
521 dead cells from the analysis, as in the absence of permeabilization it only stains dead
522 cells. Gates for tdTomato fluorescence were drawn based on a negative control
523 consisting of BC-3 cells that lack the reporter. BC-3 cells lacking the reporter were
524 treated in the same way as the sorted reporter cells. In each experiment, about $80x10^6$
525 cells were sorted. $3x10^6$ tdTomato+ and $12x10^6$ tdTomato- cells were collected in each
526 experiment. Sorted cells were pelleted and resuspended in 1 mL of Phosphate Buffer
527 Saline (PBS). 100 μL of cell suspension were used for RNA extraction and 900 μL for
528 protein extraction. Bulk controls were prepared in parallel using 4 mL of BC-3-IFN-βp-

529 tdTomato cells seeded at a density of $5x10^5$ cells/mL and treated with TPA, IDN-6556,
530 anti-IFN antibodies, TBK, or cGAS inhibitors (or corresponding vehicle) as indicated for
531 2 days. The bulk control cells were pelleted and resuspended in 1 mL of PBS. 50 µL of
532 cell suspension were used for RNA extraction, 450 µL for protein extraction, and 500 µL
533 for flow cytometry to determine KSHV reactivation efficiency.
534
535 *RT-qPCR*
536 RNA samples were collected from BC-3 or BC-3-IFN-βp-tdTomato cells reactivated for
537 2 days as described above or treated with vehicle. For experiments involving sorting, a
538 fraction of the sorted cells was used as described in the Fluorescence-activated cell
539 sorting section. For experiments not involving sorting, 4 mL of BC-3/ BC-3-IFN-βp-
540 tdTomato cells were collected as described in the same section for bulk control
541 samples. In both cases, cells to be lysed were pelleted by centrifugation and
542 resuspended in RNA lysis buffer (Zymo research). Total RNA was extracted using the
543 Quick-RNA MiniPrep kit (Zymo research) following the manufacturer's protocol. cDNA
544 was prepared using an iScript cDNA synthesis kit (Bio-Rad) following the
545 manufacturer's protocol. Real-time quantitative PCR (RT-qPCR) was performed using
546 iTaq Universal SYBR green Supermix (Bio-Rad) following the manufacturer's protocol in
547 CFX Duet Real-Time PCR System (Bio-Rad). No-template and no-RT controls were
548 included in each replicate and experiments were only included if these controls showed
549 negligible amplification rates. In all cases, target mRNA levels were normalized to levels
550 of 18S rRNA as an internal standard. CFX Maestro software was used to analyze the
551 data. Primers specific for each gene:

Target	Forward 5' → 3'	Reverse 5' → 3'	ref
Human IFN-β	GTCAGAGTGGAAATCCTAAG	ACAGCATCTGCTGGTTGAAG	(73)
Human 18S rRNA	GTAACCCGTTGAACCCCATT	CCATCCAATCGGTAGTAGCG	(74)
Human MxA	ATCCTGGGATTTTGGGGCTT	CCGCTTGTCGCTGGTGTCG	(75)
tdTomato	ACATCCCCGATTACAAGAAGC	TTGTAGATCAGCGTGCCGTC	(76)
Human IFN-λ1	CGCCTTGGAAGAGTCACTCA	GAAGCCTCAGGTCCCAATTC	(77)

552

553 *Protein analysis*

554 Protein samples were collected from BC-3/BC-3-IFN-βp-tdTomato cells reactivated for 2
555 days as described above or treated with vehicle. For experiments involving sorting, a
556 fraction of the sorted cells was used as described in the Fluorescence-activated cell
557 sorting section. For samples not involving in sorting, 4 mL of BC-3/ BC-3-IFN-βp-
558 tdTomato cells were used and collected as described for bulk control samples in that
559 section. In both cases, cells to be lysed were pelleted by centrifugation and
560 resuspended in an NP-40-only buffer (50 mM Tris-HCl pH 7.4, 150 mM NaCl, 1 mM
561 EDTA, 0.5% NP-40) supplemented with a broad-spectrum protease inhibitor mixture
562 (Thermo Scientific A32955) and a broad-spectrum phosphatase inhibitor mixture
563 (Thermo Scientific A32957). Protein concentration was determined by Bradford method
564 (Bio-Rad 5000006). Between 10 and 20 µg of protein were loaded on each gel. Laemmli
565 buffer (Bio-Rad) was added to samples before incubation at 95°C for 5 min. Samples
566 were separated by SDS-PAGE and transferred to polyvinylidene difluoride membranes
567 (PVDF; Fisher Scientific IPFL00010) using the semi-dry Trans-Blot Turbo Transfer
568 System (Bio-Rad). Membranes were blocked in 5% bovine serum albumin (BSA; Fisher
569 BioReagents BP1600-100) in Tris-Buffer Saline with 0.1% Tween (TBST). All antibodies
570 used were diluted 1:1000 in 5% BSA in TBST for staining. The following Cell Signaling
571 Technologies antibodies were used: IRF3 (D6I4C, no.11904), phospho-IRF3 Ser386

572 (E7J8G, no.37829), TBK1 (D1B4, no.3504), phospho-TBK1 Ser172 (D52C2, no.5483),
573 ATF2 (D4L2X, no.35031), c-Jun (60A8, no.9165), NF-κB p65/RelA (D14E12, no.8242),
574 phospho-NF-κB p65/RelA Ser536 (93H1, no.3303). In addition, antibodies against β-
575 actin (Abcam, ab8229) were used to stain for loading controls. Secondary horseradish
576 peroxidase (HRP)-conjugated antibodies (goat anti-rabbit and rabbit anti-goat IgG) were
577 purchased from Southern Biotechnology (no.4030-05, no.OB6106-05) and used at
578 1:5000 in 5% BSA in TBST. All membranes were exposed using SuperSignal West Pico
579 PLUS Chemiluminescent Substrate (Thermo Scientific) and imaged with an iBright
580 FL1000 imaging system (Thermo Scientific). Protein quantification from western images
581 was done using Image J (78).
582
583 *Flow cytometry analysis*
584 BC-3-IFN-βp-tdTomato cells were fixed with 4% paraformaldehyde (PFA; Electron
585 Microscopy Sciences) in PBS for 15 min at room temperature and washed twice with
586 PBS. Then, the cells were permeabilized by incubating in ice cold 90% methanol diluted
587 in 0.5% BSA in PBS for 5 mins on ice and washed twice with 0.5% BSA in PBS. For
588 measurements of IFN-βp-tdTomato reporter activity, cells were then filtered through a
589 35 μm strainer (Chemglass Life Sciences CLS4380009) and analyzed. For assessment
590 of reactivation efficiency, cells were stained for a KSHV lytic infection marker, ORF45.
591 They were incubated with antibodies against KSHV ORF45 (Thermo Fisher MA514769)
592 at 1:100 dilution for 1 hr at room temperature, washed twice, and then stained with
593 Alexa Fluor 647 (AF647)-conjugated secondary antibody at 1:500 dilution (Thermo
594 Fisher A21236) for 30 min at room temperature in the dark. 0.5 % BSA in PBS was

595 used for all incubations and washes. Cells were collected by centrifugation at 500 x *g*
596 for 5 min between all washes/incubation. After two washes, cells were resuspended in
597 0.5% BSA in PBS and filtered as above for analysis. AF647 fluorescence and tdTomato
598 fluorescence were quantified by flow cytometry on a Thermo Fisher Attune NxT V6
599 cytometer at the UW-Madison Carbone Cancer Center Flow Cytometry Laboratory.
600 AF647 fluorescence was gated based on the corresponding latently infected and vehicle
601 (DMSO)-treated cells. tdTomato fluorescence was gated based on BC-3 cells that lack
602 the reporter system. $3x10^6$ events were collected per sample. FlowJo 10.8.2 was used
603 for the data analysis.
604
605 *Single cell RNA sequencing analysis*
606 A dataset obtained from iSLK.219 cell samples previously published in Lent, Tabtieng,
607 et al., 2022 (6) (GSE190558) was re-analyzed in the current study by extracting
608 prepared Seurat matrices and manually selecting genes of interest.
609
610 *Statistics*
611 All statistical analysis was performed using GraphPad Prism version 10.3.0 or later
612 (GraphPad Software, Boston, MA USA; www.graphpad.com). Statistical significance
613 was determined by One- or Two-way ANOVA followed by a *post hoc* multiple-
614 comparison test (Dunnett or Tukey) when multiple comparisons were required. Singular
615 outliers were identified using Grubbs' test (alpha = 0.05) for outliers, and removed from
616 Fig. 1E, F, and Fig. 3A, C, E, F. All plots represent mean +/- standard deviation. Figure

617 legends indicate the number of biological replicates used for each experiment. All
618 western blot images are representative of multiple independent biological replicates.
619

620 **Acknowledgements**

621 We thank members of the Gaglia laboratory for suggestions and feedback on the
622 project and the manuscript. We thank the University of Wisconsin Carbone Cancer
623 Center (UWCCC) Flow Cytometry Laboratory staff for technical and conceptual
624 assistance and services. This work was supported by National Institutes of Health Grant
625 R01 CA268976 to M.M.G. and by the University of Wisconsin-Madison, Office of the
626 Vice Chancellor for Research and Graduate Education with funding from the Wisconsin
627 Alumni Research Foundation. The UWCCC Flow Cytometry Laboratory is supported by
628 the UWCCC Cancer Center Grant P30 CA014520.

629 **References**

630 1. Schoggins JW, Wilson SJ, Panis M, Murphy MY, Jones CT, Bieniasz P, Rice CM. 2011.
631 A diverse array of gene products are effectors of the type I interferon antiviral response.
632 Nature 472.
633 2. Schoggins JW, Rice CM. 2011. Interferon-stimulated genes and their antiviral effector
634 functions. Curr Opin Virol 1:7.
635 3. Taft J, Bogunovic D. 2018. The Goldilocks Zone of Type I IFNs: Lessons from Human
636 Genetics. J Immunol 201:7.
637 4. González-Navajas JM, Lee J, David M, Raz E. 2012. Immunomodulatory functions of
638 type I interferons. Nat Rev Immunol 12:11.
639 5. Kobayashi KS, Flavell RA. 2004. Shielding the double-edged sword: negative regulation
640 of the innate immune system. J Leukoc Biol 75:6.
641 6. Tabtieng T, Lent RC, Kaku M, Monago Sanchez A, Gaglia MM. 2022. Caspase-
642 Mediated Regulation and Cellular Heterogeneity of the cGAS/STING Pathway in
643 Kaposi's Sarcoma-Associated Herpesvirus Infection. mBio e0244622.
644 7. Hamele CE, Russell AB, Heaton NS. 2022. In Vivo Profiling of Individual Multiciliated
645 Cells during Acute Influenza A Virus Infection. J Virol 96.
646 8. Hein MY, Weissman JS. 2022. Functional single-cell genomics of human
647 cytomegalovirus infection. Nat Biotechnol 40:11.
648 9. Fiege JK, Thiede JM, Nanda HA, Matchett WE, Moore PJ, Montanari NR, Thielen BK,
649 Daniel J, Stanley E, Hunter RC, Menachery VD, Shen SS, Bold TD, Langlois RA. 2021.
650 Single cell resolution of SARS-CoV-2 tropism, antiviral responses, and susceptibility to
651 therapies in primary human airway epithelium. PLoS Pathog 17.
652 10. Sun J, Vera JC, Drnevich J, Lin YT, Ke R, Brooke CB. 2020. Single cell heterogeneity in
653 influenza A virus gene expression shapes the innate antiviral response to infection.
654 PLoS Pathog 16.

655 11. Russell AB, Elshina E, Kowalsky JR, Te Velthius AJW, Bloom JD. 2019. Single-Cell
656 Virus Sequencing of Influenza Infections That Trigger Innate Immunity. J Virol 93.
657 12. Drayman N, Patel P, Vistain L, Tay S. 2019. HSV-1 single-cell analysis reveals the
658 activation of anti-viral and developmental programs in distinct sub-populations. Elife 8.
659 13. O'Neal JT, Upadhyay A, Wolabaugh A, Patel NB, Bosinger SE, Suthar MS. 2019. West
660 Nile Virus-Inclusive Single-Cell RNA Sequencing Reveals Heterogeneity in the Type I
661 Interferon Response within Single Cells. J Virol 93.
662 14. Russell AB, Trapnell C, Bloom JD. 2018. Extreme heterogeneity of influenza virus
663 infection in single cells. Elife 7.
664 15. Killip MJ, Jackson R, Pérez-Cidoncha M, Fodor E, Randall RE. 2017. Single-cell studies
665 of IFN-β promoter activation by wild-type and NS1-defective influenza A viruses. J Gen
666 Virol 98:7.
667 16. Pérez-Cidoncha M, Killip MJ, Oliveros JC, Asensio VJ, Fernández Y, Bengoechea JA,
668 Randall RE, Ortín J. 2014. An unbiased genetic screen reveals the polygenic nature of
669 the influenza virus anti-interferon response. J Virol 88:15.
670 17. Kallfass C, Lienenklaus S, Weiss S, Staeheli P. 2013. Visualizing the beta interferon
671 response in mice during infection with influenza A viruses expressing or lacking
672 nonstructural protein 1. J Virol 87:6.
673 18. Hu J, Nudelman G, Shimoni Y, Kumar M, Ding Y, López C, Hayot F, Wetmur JG,
674 Sealfon S. 2011. Role of cell-to-cell variability in activating a positive feedback antiviral
675 response in human dendritic cells. PLoS One 6.
676 19. Hu J, Sealfon S, Hayot F, Jayaprakash C, Kumar M, Pendleton AC, Ganee A,
677 Fernandez-Sesma A, Moran TM, Wetmur JG. 2007. Chromosome-specific and noisy
678 IFNB1 transcription in individual virus-infected human primary dendritic cells. Nucleic
679 Acids Res 35:10.

680 20. Tabtieng T, Degterev A, Gaglia MM. 2018. Caspase-Dependent Suppression of Type I
681 Interferon Signaling Promotes Kaposi's Sarcoma-Associated Herpesvirus Lytic
682 Replication. J Virol 92.
683 21. Zhao M, Zhang J, Phatnani H, Scheu S, Maniatis T. 2012. Stochastic expression of the
684 interferon-β gene. PLoS Biol 10.
685 22. Rand U, Rinas M, Schwerk J, Nöhren G, Linnes M, Kröger A, Flossdorf M, Kály-Kullai K,
686 Hauser H, Höfer T, Köster M. 2012. Multi-layered stochasticity and paracrine signal
687 propagation shape the type-I interferon response. Mol Syst Biol 8.
688 23. Panne D, Maniatis T, Harrison SC. 2007. An atomic model of the interferon-beta
689 enhanceosome. Cell 129:13.
690 24. Apostolou E, Thanos D. 2008. Virus Infection Induces NF-kappaB-dependent
691 interchromosomal associations mediating monoallelic IFN-beta gene expression. Cell
692 134:7.
693 25. Surre J, Saint-Ruf C, Collin V, Orenga S, Ramjeet M, Matic I. 2018. Strong increase in
694 the autofluorescence of cells signals struggle for survival. Sci Rep 8.
695 26. Li K, Chen Z, Kato N, Gale K, Lemon SM. 2005. Distinct poly(I-C) and virus-activated
696 signaling pathways leading to interferon-beta production in hepatocytes. J Biol Chem
697 280:9.
698 27. Guo F, Mead J, Aliya N, Wang L, Cuconati A, Wei L, Li K, Block TM, Guo JT, Chang J.
699 2012. RO 90-7501 enhances TLR3 and RLR agonist induced antiviral response. PLoS
700 One 7.
701 28. Gentili M, Kowal J, Tkach M, Satoh T, Lahaye X, Conrad C, Boyron M, Lombard B,
702 Durand S, Kroemer G, Loew D, Dalod M, Thery C, Manel N. 2015. Transmission of
703 innate immune signaling by packaging of cGAMP in viral particles. Science 349.
704 29. Day RN, Davidson MW. 2009. The fluorescent protein palette: tools for cellular imaging.
705 Chem Soc Rev 38:34.

706 30. Muzumdar MD, Tasic B, Miyamichi K, Li L, Luo L. 2007. A global double-fluorescent Cre
707 reporter mouse. Genesis 45:13.
708 31. Brulois KF, Chang H, Lee ASY, Ensser A, Wong LY, Toth Z, Lee SH, Lee HR, Myoung
709 J, Ganem D, Oh TK, Kim JF, Gao SJ, Jung JU. 2012. Construction and Manipulation of
710 a New Kaposi's Sarcoma-Associated Herpesvirus Bacterial Artificial Chromosome
711 Clone. J Virol 86.
712 32. Cohen A, Brodie C, Sarid R. 2006. An essential role of ERK signalling in TPA-induced
713 reactivation of Kaposi's sarcoma-associated herpesvirus. J Gen Virol 87:8.
714 33. Kikkawa U, Matsuzaki H, Yamamoto T. 2002. Protein kinase C delta (PKC delta):
715 activation mechanisms and functions. J Biochem 132:9.
716 34. Duquesnes N, Lezoualc'h F, Crozatier B. 2011. PKC-delta and PKC-epsilon: foes of the
717 same family or strangers? J Mol Cell Cardiol 51:9.
718 35. Menezes J, Leibold W, Klein G, Clemens G. 1975. Establishment and characterization of
719 an Epstein-Barr virus (EBC)-negative lymphoblastoid B cell line (BJA-B) from an
720 exceptional, EBV-genome-negative African Burkitt's lymphoma. Biomedicine 22:9.
721 36. Arvanitakis L, Mesri EA, Nador RG, Said JW, Asch AS, Knowles DM, Cesarman E.
722 1996. Establishment and characterization of a primary effusion (body cavity-based)
723 lymphoma cell line (BC-3) harboring kaposi's sarcoma-associated herpesvirus
724 (KSHV/HHV-8) in the absence of Epstein-Barr virus. Blood 88.
725 37. Sun Z, Xiao B, Jha HC, Lu J, Banerjee S, Robertson ES. 2014. Kaposi's sarcoma-
726 associated herpesvirus-encoded LANA can induce chromosomal instability through
727 targeted degradation of the mitotic checkpoint kinase Bub1. J Virol 88:11.
728 38. Domsic JF, Chen HS, Lu F, Marmorstein R, Lieberman PM. 2013. Molecular basis for
729 oligomeric-DNA binding and episome maintenance by KSHV LANA. PLoS Pathog 9.
730 39. Ma F, Li B, Liu S, Iyer SS, Yu Y, Wu A, Cheng G. 2015. Positive feedback regulation of
731 type I IFN production by the IFN-inducible DNA sensor cGAS. 194 4:10.

732 40. Onoguchi K, Yoneyama M, Takemura A, Akira S, Taniguchi T, Namiki H, Fujita T. 2007.
733 Viral infections activate types I and III interferon genes through a common mechanism. J
734 Biol Chem 282:6.
735 41. Lenardo MJ, Fan CM, Maniatis T, Baltimore D. 1989. The involvement of NF-kappa B in
736 beta-interferon gene regulation reveals its role as widely inducible mediator of signal
737 transduction. Cell 57:8.
738 42. Wathelet MG, Lin CH, Parekh BS, Ronco LV, Howley PM, Maniatis T. 1998. Virus
739 infection induces the assembly of coordinately activated transcription factors on the IFN-
740 beta enhancer in vivo. Mol Cell 1:11.
741 43. Maniatis T, Falvo JV, Kim TH, Kim TK, Lin CH, Parekh BS, Wathelet MG. 1998.
742 Structure and function of the interferon-beta enhanceosome. Cold Spring Harb Symp
743 Quant Biol 63:12.
744 44. Iversen MB, Paludan SR. 2010. Mechanisms of type III interferon expression. J
745 Interferon Cytokine Res 30:6.
746 45. Holländer GA. 1999. On the stochastic regulation of interleukin-2 transcription. Semin
747 Immunol 11:11.
748 46. Guo L, Hu-Li J, Paul WE. 2004. Probabilistic regulation of IL-4 production in Th2 cells:
749 accessibility at the Il4 locus. Immunity 20:11.
750 47. Guo L, Hu-Li J, Paul WE. 2005. Probabilistic regulation of IL-4 production. J Clin
751 Immunol 25:9.
752 48. Kelly BL, Locksley RM. 2000. Coordinate regulation of the IL-4, IL-13, and IL-5 cytokine
753 cluster in Th2 clones revealed by allelic expression patterns. J Immunol 165:5.
754 49. Calado DP, Paixão T, Holmberg D, Haury M. 2006. Stochastic monoallelic expression of
755 IL-10 in T cells. J Immunol 177:7.
756 50. Ishikawa H, Barber GN. 2008. STING is an endoplasmic reticulum adaptor that
757 facilitates innate immune signalling. Nature 455:5.

758 51. Balka KR, Louis C, Saunders TL, Smith AM, Calleja DJ, D'Silva DB, Moghaddas F,
759 Tailler M, Lawlor KE, Zhan Y, Burns CJ, Wicks IP, Miner JJ, Kile BT, Masters SL, De
760 Nardo D. 2020. TBK1 and IKKε Act Redundantly to Mediate STING-Induced NF-κB
761 Responses in Myeloid Cells. Cell Rep 31.
762 52. Sakurai H, Chiba H, Miyoshi H, Sugita T, Toriumi W. 1999. IkappaB kinases
763 phosphorylate NF-kappaB p65 subunit on serine 536 in the transactivation domain. J
764 Biol Chem 274:4.
765 53. Mattioli I, Sebald A, Bucher C, Charles RP, Nakano H, Doi T, Kracht M, Schmitz ML.
766 2004. Transient and selective NF-kappa B p65 serine 536 phosphorylation induced by T
767 cell costimulation is mediated by I kappa B kinase beta and controls the kinetics of p65
768 nuclear import. J Immunol 172:9.
769 54. Buss H, Dörrie A, Schmitz ML, Hoffmann E, Resch K, Kracht M. 2004. Constitutive and
770 interleukin-1-inducible phosphorylation of p65 NF-{kappa}B at serine 536 is mediated by
771 multiple protein kinases including I{kappa}B kinase (IKK)-{alpha}, IKK{beta},
772 IKK{epsilon}, TRAF family member-associated (TANK)-binding kinase 1 (TBK1), and an
773 unknown kinase and couples p65 to TATA-binding protein-associated factor II31-
774 mediated interleukin-8 transcription. J Biol Chem 279:10.
775 55. Sakurai H, Miyoshi H, Toriumi W, Sugita T. 1999. Functional interactions of transforming
776 growth factor beta-activated kinase 1 with IkappaB kinases to stimulate NF-kappaB
777 activation. J Biol Chem 274:8.
778 56. Parekh N, Winship D, Dis EV, Stetson DB. 2024. Regulation and Dynamics of IFN-β
779 Expression Revealed with a Knockin Reporter Mouse. J Immunol 213:11.
780 57. Shalek AK, Satija R, Shuga J, Trombetta JJ, Gennert D, Lu D, Chen P, Gertner RS,
781 Gaublomme JT, Yosef N, Schwartz S, Fowler B, Weaver S, Wang J, Wang X, Ding R,
782 Raychowdhury R, Friedman N, Hacohen N, Park H, May AP, Regev A. 2014. Single-cell
783 RNA-seq reveals dynamic paracrine control of cellular variation. Nature 510:7.

784 58. Strahle L, Garcin D, Kolakofsky D. 2006. Sendai virus defective-interfering genomes and
785 the activation of interferon-beta. Virology 351:11.
786 59. Johnston MD. 1981. The characteristics required for a Sendai virus preparation to
787 induce high levels of interferon in human lymphoblastoid cells. J Gen Virol 56:10.
788 60. Patil S, Fribourg M, Ge Y, Batish M, Tyagi S, Hayot F, Sealfon S. 2015. Single-cell
789 analysis shows that paracrine signaling by first responder cells shapes the interferon-β
790 response to viral infection. Sci Signal 8.
791 61. Hwang SY, Hur KY, Kim JR, Cho KH, Kim SH, Yoo JY. 2013. Biphasic RLR-IFN-β
792 response controls the balance between antiviral immunity and cell damage. J Immunol
793 190:9.
794 62. Zawatzky R, Maeyer ED, Maeyer-Guignard JD. 1985. Identification of individual
795 interferon-producing cells by in situ hybridization. PNAS 82:5.
796 63. Enoch T, Zinn K, Maniatis T. 1986. Activation of the human beta-interferon gene
797 requires an interferon-inducible factor. Mol Cell Biol 6:10.
798 64. Bhowmik D, Tian Y, Wang B, Zhu F, Yin Q. 2022. Structural basis of higher order
799 oligomerization of KSHV inhibitor of cGAS. PNAS 199.
800 65. Zhang G, Chan B, Samarina N, Abere B, Weidner-Glunde M, Buch A, Pich A,
801 Brinkmann MM, Schulz TF. 2016. Cytoplasmic isoforms of Kaposi sarcoma herpesvirus
802 LANA recruit and antagonize the innate immune DNA sensor cGAS. PNAS 133.
803 66. Yu K, Tian H, Deng H. 2020. PPM1G restricts innate immune signaling mediated by
804 STING and MAVS and is hijacked by KSHV for immune evasion. Sci Adv 6.
805 67. Ma Z, Jacobs SR, West JA, Stopford C, Zhang Z, Davis Z, Barber GN, Glausinger BA,
806 Dittmer DP, Damania B. 2015. Modulation of the cGAS-STING DNA sensing pathway by
807 gammaherpesviruses. PNAS 112.

808 68. Joo CH, Shin YC, Gack M, Wu L, Levy D, Jung JU. 2007. Inhibition of Interferon
809 Regulatory Factor 7 (IRF7)-Mediated Interferon Signal Transduction by the Kaposi's
810 Sarcoma-Associated Herpesvirus Viral IRF Homolog vIRF3. J Virol 81:10.
811 69. Hwang SW, Kim D, Jung JU, Lee HR. 2017. KSHV-encoded viral interferon regulatory
812 factor 4 (vIRF4) interacts with IRF7 and inhibits interferon alpha production. Biochem
813 Biophys Res Commun 486:6.
814 70. Aresté C, Mutocheluh M, Blackbourn DJ. 2009. Identification of caspase-mediated decay
815 of interferon regulatory factor-3, exploited by a Kaposi sarcoma-associated herpesvirus
816 immunoregulatory protein. J Biol Chem 284:13.
817 71. Burysek L, Yeow WS, Lubyova B, Kellum M, Schafer SL, Huang YQ, Pitha PM. 1999.
818 Functional Analysis of Human Herpesvirus 8-Encoded Viral Interferon Regulatory Factor
819 1 and Its Association with Cellular Interferon Regulatory Factors and p300. J Virol 73.
820 72. Lin R, Genin P, Mamane Y, Sgarbanti M, Battistini A, Harrington WJ, Barber GN, Hiscott
821 J. 2001. HHV-8 encoded vIRF-1 represses the interferon antiviral response by blocking
822 IRF-3 recruitment of the CBP/p300 coactivators. Oncogene 20:12.
823 73. Yang Q, Elz AE, Panis M, Liu T, Nilsson-Payant BE, Blanco-Melo D. 2023. Modulation of
824 Influenza A virus NS1 expression reveals prioritization of host response antagonism at
825 single-cell resolution. Front Microbiol 14.
826 74. Schmittgen TD, Zakrajsek BA. 2000. Effect of experimental treatment on housekeeping
827 gene expression: validation by real-time, quantitative RT-PCR. J Biochem Biophys
828 Methods 46:11.
829 75. Zhu FX, Sathish N, Yuan Y. 2010. Antagonism of host antiviral responses by Kaposi's
830 sarcoma-associated herpesvirus tegument protein ORF45. PLoS One 5.
831 76. Valny M, Honsa P, Waloschkova E, Matuskova H, Kriska J, Kirdajova D, Androvic P,
832 Valihrach L, Kubista M, Anderova M. 2018. A single-cell analysis reveals multiple roles
833 of oligodendroglial lineage cells during post-ischemic regeneration. Glia 66:14.

834 77. Ank N, West H, Bartholdy C, Eriksson K, Thomsen AR, Paludan S. 2006. Lambda
835 interferon (IFN-lambda), a type III IFN, is induced by viruses and IFNs and displays
836 potent antiviral activity against select virus infections in vivo. J Virol 80:9.
837 78. Stael S, Miller LP, Fernández-Fernández ÁD, Van Breusegem F. 2022. Detection of
838 Damage-Activated Metacaspase Activity by Western Blot in Plants. Methods Mol Biol
839 2447:11.
840

841 **Figure Legends**

842 **Figure 1. An IFN-β-promoter driven fluorescent reporter allows isolation of cells**
843 **expressing high and low levels of IFN-β. A.** Diagram of the IFN-βp-tdTomato
844 reporter. Two copies of the 303 bp minimal promoter sequence for the human IFNB1
845 gene were cloned in front of the tdTomato fluorophore. This cassette was then
846 introduced in BC-3 cells via lentiviral transduction for stable integration. **B-G.** BC3-IFN-
847 βp-tdTomato reporter cells were treated with 20 ng/mL TPA for 48 hours to induce the
848 lytic cycle ("lytic (+TPA)"). Where indicated, the cells were also treated with 10 μM of the
849 pan-caspase inhibitor IDN-6556 ("casp-i") and/or with a cocktail of antibodies against
850 type I IFNs and their receptor ("anti-IFN Abs") at 1:2000 dilution. IFN-β and tdTomato
851 mRNA levels were measured by RT-qPCR and normalized to 18S rRNA. For **B** and **E**,
852 IFN-β mRNA levels are normalized to the lytic+casp-i sample. For **C**, **D**, **F**, and **G,** the
853 lytic+casp-i (**C, D**) or the lytic+casp-i+anti-IFN Ab (**F, G**) samples were sorted based on
854 tdTomato expression and the fold enrichment in IFN-β and tdTomato RNA levels
855 compared to unsorted ("bulk") samples is plotted in $\log_2$ scale. ns = $p>0.05$, ** = $p<0.01$,
856 *** = $p<0.001$, **** = $p<0.0001$. One-Way ANOVA followed by Dunnett's (B, E) or
857 Tukey's (C, D, F, G) post hoc multiple comparisons test. n=6 for B-D. n=4 for E-G.
858

859 **Figure 2. Treatment with TPA and caspase inhibitors does not induce IFN**
860 **signaling in uninfected B cells.** KSHV-negative BJAB cells were treated with 20 ng/ml
861 TPA and/or 10 μM of the pan-caspase inhibitor IDN-6556 ("casp-i") for 48 hrs. BC-3
862 cells treated with TPA and IDN-6556 were used as a positive control for induction of
863 type I and III IFNs. IFN-β (**A**) and IFN-λ1 (**B**) mRNA levels were measured by qRT-PCR

and normalized to 18S rRNA. The expression levels are normalized to the TPA and IDN-6556-treated BC-3 sample for each experiment. **** = p<0.0001, One-Way ANOVA followed by Dunnett's post hoc multiple comparisons test. n=4.

Figure 3. IFN-λ1 and IFN-β are coordinately induced in a subset of cells, pointing to heterogeneity in the induction pathway rather than stochastic noise in expression. A. Diagram of coordinate induction of IFN-β and IFN-λ. In first responder cells, IFN-β and IFN-λ are induced in response to infection or lytic reactivation downstream of PRRs, whereas in secondary responder cells, IFNs and ISGs such as MxA are induced in response to signaling downstream of IFN receptors. **B-I.** BC3-IFN-βp-tdTomato reporter cells were treated with 20 ng/ml TPA for 48 hours to induce the lytic cycle ("lytic (+TPA)"). Where indicated, the cells were also treated with 10 μM of the pan-caspase inhibitor IDN-6556 ("casp-i") and/or a cocktail of antibodies against type I IFNs and their receptor ("anti-IFN Abs") at 1:2000 dilution. IFN-λ1 (**B-E**) and MxA (**F-I**) mRNA levels were measured by RT-qPCR and normalized to 18S rRNA. In **B**, **D**, **F**, and **H,** IFN-λ1 and MxA mRNA levels are plotted relative to the lytic+casp-i sample. In **C, E, G, and I,** the lytic+casp-i (**C, G**) or the lytic+casp-i+anti-IFN Abs (**E, I**) samples were sorted based on tdTomato expression and the fold enrichment in IFN-λ1 (**C**) and MxA (**G**) mRNA levels compared to unsorted ("bulk") samples are plotted in $\log_2$ scale. ns = p>0.05, * = p<0.05, ** = p<0.01, **** = p<0.0001, One-Way ANOVA followed by Dunnett's (A, C, E, G) or Tukey's (B, D, F, H) post hoc multiple comparisons test. n=6 for A, B, E, F. n=4 for C, D, G, H.

887 **Figure 4. TBK1 and IRF3 are necessary but not sufficient to direct IFN-β**
888 **expression, as they are activated even in cells with low IFN-β expression.** BC3-
889 IFN-βp-tdTomato reporter cells were treated with 20 ng/ml TPA for 48 hours to induce
890 the lytic cycle ("lytic (+TPA)"). Where indicated, the cells were also treated with 10 μM of
891 the pan-caspase inhibitor IDN-6556 ("casp-i"), 10 μM of the TBK1 inhibitor MRT76307
892 ("TBK1i"), 10 μM of the cGAS inhibitor G140 ("cGASi"), and/or a cocktail of antibodies
893 against type I IFNs and their receptor ("anti-IFN Abs") at 1:2000 dilution. **A.** IFN-β
894 mRNA levels were measured by qRT-PCR and normalized to 18S rRNA. The
895 expression levels are normalized to "untreated" lytic+casp-i samples that did not receive
896 TBK1i or cGASi for each experiment. n=3. **** = $p<0.0001$. Two-Way ANOVA followed
897 by Tukey's post hoc multiple comparisons test. **B-H.** Protein lysates were probed for
898 phosphorylated IRF3 (Ser386), total IRF3, phosphorylated TBK1 (Ser172), total TBK1,
899 and β-actin as a loading control. As a positive control for IRF3 and TBK1
900 activation/phosphorylation, A549 cells were treated with poly(I:C) for 6 and 48 hours
901 before protein lysates were collected. Protein was isolated from treated BC3-IFN-βp-
902 tdTomato reporter cells without sorting ("bulk"), or after sorting the lytic+casp-i (**B-D**) or
903 lytic+casp-i+anti-IFN Abs (**E-H**) sample based on tdTomato expression. Western blot for
904 phosphorylated TBK1 (**C, F**) and phosphorylated IRF3 (**D, G**) were quantified by
905 normalizing the density of phosphorylated protein to unphosphorylated protein bands
906 per lane for bulk lytic+casp-i treated samples and sorted tdTomato+ and tdTomato-
907 samples. **H.** KSHV-negative BJAB cells were treated with vehicle, 20 ng/ml TPA, and/or
908 10 μM of the pan-caspase inhibitor IDN-6556 ("casp-i") for 48 hours. Protein was

909 isolated and stained for phosphorylated TBK1, total TBK1, phosphorylated IRF3, and
910 total IRF3. Images shown are representative of 3 replicates (**B**, **E**) or 2 replicates (**H**).
911
912 **Figure 5. Levels of the AP-1 subunit ATF2 and phosphorylation of the NF-κB**
913 **subunit RelA are higher in cells with high IFN-β expression. A.** Diagram of the IFN-
914 β enhanceosome and its position on the IFN-β promoter. In the IFN-β enhanceosome,
915 NF-κB is composed of subunits NFKB1 (p50) and RelA, and AP-1 is composed of
916 subunits ATF2 and c-Jun. **B-C.** Re-analysis of single-cell RNA sequencing (scRNA-seq)
917 data in Tabtieng, Lent, et al 2022. iSLK.219 cells were treated with 1 μg/mL doxycycline
918 for 4 days to induce the lytic cycle ("lytic"). The cells were also treated with 10 μM of the
919 pan-caspase inhibitor IDN-6556 ("casp-i"), as well as a mixture of antibodies against
920 type I IFNs and its receptor ("anti-IFN Abs") (**C** only) to block IFN-β paracrine signaling.
921 The average mRNA levels of genes in the IFN-β enhanceosome from the scRNA-seq
922 data are shown for each of the 12 clusters of cells identified by the original analysis
923 (indicated by different colors above the heatmap). Clusters were classified as "lytic" or
924 "latent" based on the pattern of viral genes they expressed. The "lytic IFN-β-positive"
925 clusters were further separated into two groups based on the IFN-β status of individual
926 cells. **D-F, I-J.** BC3-IFN-βp-tdTomato reporter cells were treated with 20 ng/ml TPA for
927 48 hours to induce the lytic cycle ("lytic (+TPA)"), 10 μM of the pan-caspase inhibitor
928 IDN-6556 ("casp-i"), and/or a cocktail of antibodies against type I IFNs and their
929 receptor ("anti-IFN Abs") to block IFN-β paracrine signaling. Protein was isolated from
930 BC3-IFN-βp-tdTomato reporter cells without sorting ("bulk"), or after sorting the
931 lytic+casp-i+anti-IFN Abs based on tdTomato expression. Western blots were probed

932 for ATF2, c-Jun (**D**), or total RelA and phosphorylated RelA (Ser536) (**I**) or β-actin as a
933 loading control. Levels of ATF2 (**E**) and c-Jun (**F**) in sorted samples were quantified
934 from the western blots, normalized to β-actin, and plotted relative to bulk lytic+casp-i+
935 anti-IFN Abs samples. Levels of phosphorylated RelA (Ser536) (**J**) were quantified by
936 normalizing to total RelA and plotted relative to bulk lytic+casp-i+ anti-IFN Abs samples.
937 **G, H, K.** KSHV-negative BJAB cells were treated with vehicle, 20 ng/ml TPA and/or 10
938 μM of the pan-caspase inhibitor IDN-6556 ("casp-i") for 48 hrs. Protein was isolated and
939 stained for ATF2 (**G**), c-Jun (**H**), phosphorylated (Ser536) and total RelA (**K**), and β-
940 actin as a loading control. Images are representative of 4 replicates (**D**), 3 replicates (**I**),
941 or 2 replicates (**G, H, K**). ns = $p>0.05$, * = $p<0.05$, ** = $p<0.01$, One-Way ANOVA
942 followed by Tukey's post hoc multiple comparisons test.
943
944 **Figure 6. Model of regulation of heterogeneous IFN-β expression by components**
945 **of the IFN-β enhanceosome.** *(Left)* In the rare cells that induce IFN-β during viral
946 infection as "first responders", there are high levels of the AP-1 factor ATF2 and both
947 the NF-κB subunit RelA and IRF3 become phosphorylated in response to infection. This
948 results in the formation of the IFN-β enhanceosome and in IFN-β and IFN-λ1
949 transcription. *(Right)* In the majority of virally infected cells, there are lower amounts of
950 ATF2, and RelA is not phosphorylated during infection. While IRF3 is still activated, the
951 full IFN-β enhanceosome does not form and IFN-β and IFN-λ1 are not induced.